

University of Northern Colorado

Scholarship & Creative Works @ Digital UNC

Master's Theses

Student Work

5-1-2021

Exploring the Neurochemical Basis for Toluene-Induced Alterations in Accumbal Dopamine Neurotransmission

Kristofer Reiser

University of Northern Colorado

Follow this and additional works at: <https://digscholarship.unco.edu/theses>

Recommended Citation

Reiser, Kristofer, "Exploring the Neurochemical Basis for Toluene-Induced Alterations in Accumbal Dopamine Neurotransmission" (2021). *Master's Theses*. 199.

<https://digscholarship.unco.edu/theses/199>

This Thesis is brought to you for free and open access by the Student Work at Scholarship & Creative Works @ Digital UNC. It has been accepted for inclusion in Master's Theses by an authorized administrator of Scholarship & Creative Works @ Digital UNC. For more information, please contact Nicole.Webber@unco.edu.

UNIVERSITY OF NORTHERN COLORADO

Greeley, Colorado

The Graduate School

EXPLORING THE NEUROCHEMICAL BASIS FOR
TOLUENE-INDUCED ALTERATIONS IN
ACCUMBAL DOPAMINE
NEUROTRANSMISSION

A Thesis Submitted in Partial Fulfillment
of the Requirements for the Degree of
Master of Science

Kristofer Felix Kintner Reiser

College of Natural and Health Sciences
Department of Chemistry and Biochemistry

May 2021

This Thesis is by: Kristofer Felix Kintner Reiser

Entitled: *Exploring the Neurochemical Basis for Toluene-Induced Alterations in Accumbal Dopamine Neurotransmission*

has been approved as meeting the requirement for the Degree of Master of Science in the College of Natural and Health Sciences in the Department of Chemistry.

Accepted by the Thesis Committee:

Dr. Aaron K. Apawu PhD, Chair

Dr. Murielle Watzky PhD, Committee Member

Dr. Patrick Burns PhD, Committee Member

Accepted by the Graduate School:

Jeri-Anne Lyons, Ph.D.
Dean of the Graduate School
Associate Vice President for Research

ABSTRACT

Reiser, Kristofer. *Exploring the Neurochemical Basis for Toluene-Induced Alterations in Accumbal Dopamine Neurotransmission*. Unpublished Master of Science Thesis, University of Northern Colorado, 2021.

Inhalants as environmental contaminants or recreational drugs pose a considerable health concern, but little is known about their mode of action. In 2011, a study from the National Institute for Drug Addiction revealed that an estimate of 21.7 million people aged 12 or older have used inhalants that contain high concentrations of volatile organic compounds, primarily toluene. These compounds can have debilitating impact on brain chemistry. While the impact of toluene on the central dopamine reward pathway has been already reported, the exact mechanism underlining the effect of toluene is still obscure. Towards this goal, the present work seeks to unravel how toluene affects the dopamine system in the nucleus accumbens, a region implicated in addiction. Following the exposure of 63 mice to toluene inhalation for 30 minutes each day on seven consecutive days, slice fast scan cyclic voltammetry (FSCV) with carbon fiber microelectrodes was utilized to measure baseline dopamine release. The impact of toluene on the dopamine neurotransmission was further assessed by examining D2 receptor distribution using immunocytochemistry. Finally, x-ray fluorescence was used to quantify potassium, calcium, iron, copper, and zinc; elements used as secondary messengers in neurons. The combination of the electroanalytical, immunoassays, and spectroscopy shows toluene induced dysregulation in dopamine neurotransmission that could be the result of oxidative damage to neurons in the nucleus accumbens.

TABLE OF CONTENTS

CHAPTER 1 INTRODUCTION	1
1.1 Research Objectives.....	4
CHAPTER 2 LITERATURE REVIEW	7
2.1 Inhalants.....	7
2.2 Overview of Neurotransmission	7
2.3 Dopamine Synthesis and Signaling Pathways	9
2.4 Neural Basis of Addiction.....	13
2.5 Fast Scan Cyclic Voltammetry	15
2.6 X-Ray Fluorescence (XRF) Spectrometry	18
CHAPTER 3 METHODOLOGY	20
3.1 Toluene Exposure Paradigm.....	20
3.2 Verification of Toluene Concentration in the Chamber Using Fourier Transform Infrared (FTIR) Spectroscopy.....	22
3.3 Slice Fast Scan Cyclic Voltammetry (FSCV) Measurement of Dopamine Release in the Nucleus Accumbens.....	22
3.4 Measurement of Dopamine D2 Receptor Distribution Using Immunocytochemistry	23
3.5 X-Ray Fluorescence Spectrometric Measurements of Metals in Brain Tissues.....	24
3.6 Data Analyses	24

CHAPTER 4 RESULTS	28
4.1 Verification of Toluene Concentration in the Exposure Chamber Using Fourier Transform Infrared Spectroscopy	28
4.2 Slice FSCV Measurement of Dopamine Release in the Nucleus Accumbens	30
4.3 Measurement of Dopamine D2 Receptor Distribution Using Immunocytochemistry	31
4.4 X-Ray Fluorescence Spectrometric Measurements of Biometals in Brain Tissue	34
CHAPTER 5 DISCUSSION.....	40
5.1 Effect of Chronic Toluene Inhalation on Dopamine Release in the Nucleus Accumbens.....	40
5.2 The Possible Role of D2 Receptors in Toluene- Induced Changes in the Nucleus Accumbens.....	41
5.3 The Role of Biometal Ion Cofactors in Toluene’s Action on the Dopamine System	43
5.4 Conclusion	45
REFERENCES	47
APPENDIX A IMMUNOCYTOCHEMISTRY IMAGES	58
APPENDIX B INSTITUTIONAL ANIMAL CARE AND USE COMMITTEE APPROVAL	60

LIST OF FIGURES

Figure 1. Dopamine synthesis pathway	10
Figure 2. Cartoon of dopamine release in synapse showing vesicles, exocytosis, recycling and target protein interaction at the post synaptic terminal.....	11
Figure 3. Dopaminergic pathways in the A) human and B) rodent brain. The pathways shown are tuberoinfundibular (pink), mesolimbic (blue), mesocortical (yellow), and nigrostriatal (orange.).....	13
Figure 4. Fast scan cyclic voltammetry. (A) Applied waveform (B) Cyclic voltammogram (C) 3-D pseudo color plot.	17
Figure 5. Schematic of slice FSCV. The potentiostat both controls brain stimulation through the neurolog device as well as records the evoked response through the working and reference electrodes The brain slice is kept viable by mimicking conditions in intact brain. Brain slices are constantly perfused with warm oxygenated aCSF.....	18
Figure 6. Schematic of showing the principles behind X-ray fluorescence spectrometry. Incident radiation ejects an electron in an inner shell of an atom. Outer electrons fill the hole and fluoresce a photon to lose the appropriate energy.....	19
Figure 7. Schematic of XRF Instrumentation. X-Rays are produced from a high voltage laser. A monochromator is used to select a narrow range of suitable wavelengths before reflecting radiation on to the sample. Most of the x-radiation continues past the sample and only a fraction is detected.	19
Figure 8. Chronic Toluene exposure protocol.	20

Figure 9. Toluene exposure chamber constructed from a 26.5 L Pyrex jar (left) and fitted with an air-tight lid (right.) Toluene is introduced to the sealed chamber through the port (A) and dispensed onto filter paper in front of a fan (B) to expedite evaporation and circulation. Gas samples for FTIR were taken from (C). The entire exposure chamber is housed in a fume hood..... 21

Figure 10. Electrode placement for slice FSCV. The working electrode has 50 μm of exposed carbon fiber which is inserted into the brain slice approximately 150 μm from the two pronged stimulating electrode..... 23

Figure 11. Identification of nucleus accumbens core and shell for ICC analysis..... 26

Figure 12. (A) Coronal section, bregma +1.18 mm, labeling anterior commissure in red, nucleus accumbens core in blue, and nucleus accumbens shell in green. (Paxinos & Franklin, 2001). (B) stitched image of transmitted light microscopy in coronal mouse slice (C) 40x image of Alexfluor-488 staining for D2 receptors in the nucleus accumbens (100 μm bar.) (D) Fluorescence counted as positive staining by ImageJ highlighted in red (E) Readout of receptor count from ImageJ..... 27

Figure 13. Infrared absorbance spectra of toluene in room air from 650-780 cm^{-1} 29

Figure 14. Beer's Law plot of toluene gas in room air. Extinction coefficient = $1.255 \text{ E-}5 \text{ cm}^{-1} \text{ ppm}^{-1}$, $R^2= 0.992$, intercept = -0.00246. 30

Figure 15. Evoked dopamine from control and exposed mice. (A) Male and female data combined reveal no significant difference between air control ($n=8$) and 4000 ppm toluene exposed mice ($n=5$). (B) Control male mice ($n=4$) released significantly more dopamine than any other group ($p<0.05$) but there was no significant difference between the other two groups. *denotes significance where $p = 0.05$ 31

Figure 16. (A) Coronal section, bregma +1.18 mm, labeling anterior commissure in red, nucleus accumbens core in blue, and nucleus accumbens shell in green. (Paxinos & Franklin, 2001). (B) Stitched image of coronal slice stained for D2 and visualized with Alexafluor-488 (1 mm bar). Blue and green boxes indicate counting regions for the nucleus accumbens core and shell respectively and correspond to the boxes drawn in (A). (C) An enlargement of the caudate putamen (1 mm bar) showing positive staining in bright green punctation on top of background fluorescence. 32

Figure 17. (A) The Nucleus Accumbens core (M= 10.58, n=10) had more D2 receptors per 100 μm^2 than the shell (M=4.889, n=10) for air control, $t(18)= 2.747$ $p= 0.0133$. (B) There was no significant difference in D2 receptors per 100 μm^2 within the same brain region based on treatment with air control (black), 2000 ppm (pink), or 4000 ppm (green) $F(2, 57)=3.857$, $p=0.268$. * denotes significance at $\alpha=0.05$ 33

Figure 18. XRF spectra from a control animal using a Molybdenum laser source and internal 1 ppm Gallium standard. 35

Figure 19. XRF spectra from an exposed animal using a Molybdenum laser source and internal 1 ppm Gallium standard..... 36

Figure 20. Comparisons of (A) calcium $p = 0.356$ (B) potassium $p = 0.694$ (C) iron $p = 0.187$ (D) copper $p = 0.386$ and (E) zinc $p = 0.859$ broken down by sex. No differences are significant..... 38

Figure 21. Concentration of (A) Calcium ($p= 0.075$) (B) Potassium ($p=0.252$) (C) Iron $p= 0.044$ (D) Copper ($p=0.386$), and (E) Zinc ($p= 0.374$) from XRF analysis of nucleus accumbens biopsies. All comparisons were between 10 air control animals (5 males

and 5 females except for copper where one male was removed by Q test) and 9
exposed animals (4 males and 5 females.)..... 39

Figure 22: Representative ICC staining of (A) control male and (B) 4000 ppm exposed male
nucleus accumbens core. Both images measure 300 μm wide by 600 μm tall..... 599

CHAPTER 1

INTRODUCTION

Addiction is one of the largest public health concerns facing the United States today. Illicit drug use is estimated to be the cause of 23% of the ~2.5 million annual deaths nationally (Madras & Kuhar, 2014). Inhalants are recreational drugs which produce euphoric effects from purposely inhaling the fumes from volatile organic solvents. A 2011 study conducted by the U.S. National Institute for Drug Addiction found 21.7 million Americans aged 12 and older were reported to have used inhalants at least once (National Institute on Drug Abuse, 2011). Inhalants have the highest use among ages 12 to 18 (Substance Abuse and Mental Health Services Administration, 2018). Adolescence is a critical risk period during which the timing of the first use of addictive substances is correlated to the likelihood of abuse and dependence later in life (Substance Abuse and Mental Health Services Administration, 2014). Drug misuse in general does not decline in older age groups, presenting the possibility that individuals move on to other substances as they age. As a result, there is reason to believe inhalants act as “gateway” drugs.

The prevalence of inhalant abuse is attributed to the variety of products abused and the accessibility of these products as they are cheap to purchase legally. Many products commonly abused as inhalants contain the volatile organic solvent toluene, which is a psychoactive molecule capable of euphoric and intoxicating effects (Camara-Lemarroy et al., 2015).

Electrophysiological data link euphoria associated with inhalant use to increased release of the neurotransmitter dopamine specifically in the mesolimbic pathway of the brain (Camara-Lemarroy et al., 2015). The mesolimbic pathway is a neural pathway implicated in addiction because it governs motivation and processes reward stimuli (Riegel et al., 2007). It is

rationalized that the sudden increase in dopamine release in the mesolimbic pathway caused by recreational drugs signals a highly salient and rewarding experience and creates a positive feedback loop (Woodward & Beckley, 2014). The phenomenon of non physiological dopamine release is integral to understanding the mechanism of drug addiction. Inhalants are considered addictive because of their capability to modulate dopamine release in this way (Riegel & French, 1999).

The mode of action of toluene and how the brain adapts are still not fully understood. A more detailed understanding of the molecular interactions of toluene in the brain is necessary to develop effective interventions for addiction. Therapies available today focus on minimizing adverse symptoms of withdrawal. Symptoms of toluene withdrawal include nausea, irritability, tremor, agitation, and dry mouth (Villano, 2013). Except for therapies targeting μ -opioid receptors, withdrawal medications do not manage the underlying physiological cause of cravings that make long term sobriety following drug misuse so difficult. This is due to incomplete understanding of all brain functions affected by addiction including memory, emotional processing, and motivation, combined with the difficulty of drug design and approval addressing the complexities of neurological function.

Studying changes in brain activity is done by characterizing communication between neurons. Neurons communicate by releasing neurotransmitters. Previous work has shown that acute toluene exposure in mice increases dopamine release but chronic exposure decreases dopamine release in the nucleus accumbens, a region that is integral in the mesolimbic pathway (Apawu et al., 2015, 2020). Since dopamine synthesis and release are controlled by autoreceptors via negative feedback inhibition loop, the observed attenuation following the chronic toluene exposure could be indicative of altered autoreceptor function (Beaulieu & Gainetdinov, 2011).

However, autoreceptor alteration may not be the only mechanism underlying the attenuation of dopamine release after chronic exposure. Changes can occur anywhere in the dopamine cell signaling pathway such as amount of neurotransmitter synthesized which relies on enzymes with trace metal cofactors (Grochowski et al., 2019), expression levels or activation of necessary intermediate enzymes, how neurotransmitters are packaged into vesicles, release of vesicles by calcium dependent snare proteins (Ramakrishnan et al., 2012), or the exchange of potassium during neurotransmission itself. Any of these changes could contribute the observed trend. Thus, the present research explores the mechanism(s) underlying the impact of chronic toluene inhalation on dopamine neurotransmission in the nucleus accumbens.

This investigation employed fast scan cyclic voltammetry (FSCV) to examine dopamine release in brain slices of mice chronically exposed to toluene. Additionally, the effects of toluene inhalation on the distribution of dopamine D2 autoreceptors in the nucleus accumbens was examined using immunocytochemistry. The expression of D2 autoreceptors have been tied to resilience or vulnerability of humans to addiction and may play a role in the reaction of the brain to inhalation of toluene (Volkow et al., 2006). Lastly, X-Ray Fluorescence Spectrometry used to quantify necessary cofactor biometals like potassium, calcium, iron, zinc and copper. Potassium and calcium are exchanged between neurons and extracellular space in response to an action potential. Once inside neurons, calcium influences many cell signaling processes (Brini et al., 2014). Iron is required for the conversion of tyrosine into dopamine and copper is required to for the conversion of dopamine into norepinephrine. Zinc binding can modulate function of G coupled Protein Receptors and the dopamine transport protein. Thus changes in these ion concentration may reflect changes in synthesis and transmission of the neurotransmitter (Scimemi & Beato, 2009).

A detailed understanding of how toluene impacts dopamine signaling and the mechanisms behind the brain's response to toluene inhalation will increase the collective knowledge of inhalant abuse. This knowledge has the potential to inform the development of novel therapies targeted at preventing inhalant abuse, such as lowering an individual's vulnerability to inhalant addiction, or the deleterious symptoms of withdrawal. Given that inhalant abuse is a particular problem in adolescents, the benefits of effective therapy have the potential to impact individuals well into their adult life.

1.1 Research Objectives

The recent findings by Apawu et al., 2020, describe neuroadaptation in mouse nucleus accumbens following chronic exposure to 4000 ppm toluene marked by a decrease in dopamine release but suggest that dopamine autoreceptor D3 is not involved. To further investigate the mechanism of compensation employed during chronic exposure paradigms, the present investigation focused on three main objectives.

O1 Verifying the impact of chronic toluene exposure on dopamine release.

The present objective sought to confirm the recently reported findings that chronic toluene exposure decreases evoked dopamine release in the Nucleus Accumbens. A decrease in stimulated efflux of dopamine following chronic toluene exposure could be explained by inhibition of dopamine synthesis or G protein coupled receptor inhibition of voltage gated Ca^{2+} channels. Herein, the maximum stimulated dopamine signal was expected to differ between the toluene exposed and air control mice. The brains of control and 4000 ppm toluene exposed animals were analyzed by *slice* FSCV and the concentration of dopamine evoked from the nucleus accumbens was compared between the two groups.

O2 Examining the effect of chronic toluene exposure on D2 receptors in the nucleus accumbens.

We examined what changes occur in the brain that produce the phenomenon of tolerance to toluene exposure. Because D2 receptors participate in negative feedback inhibition of dopamine release, it is important to examine their contributions. A decrease in dopamine release could be caused by a change in the quantity of D2 receptor proteins or distribution or their function. For example, increasing the number of D2 receptors could amplify their ability to inhibit dopamine release. Tolerance could also be produced by a change in function of D2 receptors. Allosteric modulators could impact the number of normally functioning proteins without changing the number physically present.

D2 autoreceptors play a significant role in modulating extracellular dopamine levels by activating a secondary messenger cascade potentially targeting decreased dopamine synthesis and subsequent release. It is plausible that chronic toluene exposure affects not only the D2 receptors levels but also the distribution across the nucleus accumbens. Thus, the present objective seeks to evaluate the D2 receptor distribution in the nucleus accumbens following chronic exposure to physiologically relevant doses (2000 and 4000 ppm) of toluene. The distribution of D2 receptors in the toluene exposed subject was compared with that of the control. Coronal slices of brain tissue were stained for dopamine receptor 2 and imaged via confocal microscopy. ImageJ software was used to count receptors in the nucleus accumbens core and shell.

- O3 Examining the impact of chronic toluene exposure on the necessary biometals and second messengers.

Another possible mechanism to the toluene-induced reduction in dopamine release previously observed could be via a decrease in dopamine synthesis, a process catalyzed by iron dependent tyrosine hydroxylase or decreased vesicle exocytosis by Ca^{2+} dependent snare proteins. Because G coupled protein receptors can act on a wide diversity of cellular signaling pathways and secondary messengers, monitoring necessary metals that can regulate cell signaling like potassium, calcium, iron, zinc, and copper can provide reinforcing evidence for which specific pathways may be elucidated. Under this objective, XRF spectrometry was used to determine the concentration of trace metals in the nucleus accumbens. Biopsies of the nucleus accumbens were lysed and homogenized, and aliquots of the lysate were analyzed for the biometals analysis.

CHAPTER 2

LITERATURE REVIEW

2.1 Inhalants

Most substances which are abused as inhalants are widely available for purchase legally and without age restriction. This includes household items which might be thought of as innocuous like rubber cement, nail polish remover, spray paint and markers. Those who abuse inhalants may inhale fumes directly from open containers or inhale through solvent soaked cloth. Inhalants can be lethal as they can cause cardiac arrhythmia and sudden death. Chronic inhalant abuse leads to encephalopathy, a permanent and disabling damage to white matter, and a dementia with characteristic cognitive deficits (Filley et al., 2004).

The major psychoactive component of most substances abused as inhalants is toluene. Toluene is colloquially described as producing a “quick drunk” effect. Once inhaled, toluene quickly crosses the blood-brain barrier and interferes with neurotransmission (Cruz et al., 2014). Headaches and slower reflexes are reported following inhalation of low concentrations (~ 200 ppm) of toluene. Confusion has also been reported at moderately higher concentrations, with euphoria reported above 800 ppm toluene inhalation.

2.2 Overview of Neurotransmission

Multipolar neurons have a cell body, which houses most organelles; dendrites, which extend a short distance from the body and receive information from other neurons; and axons, which are long tails extending towards the dendrites of other neurons. The potential at rest across the plasma membrane of a neuron sits at around -70 mV and is maintained by the Na⁺ and K⁺ ATPase pump which works against the concentration gradient. Sodium ions slowly enter, and

potassium ions slowly exit the neuron through leakage channels, raising the potential across the membrane. This is called a local potential. When sufficient sodium ions have entered the neuron to surpass -50 mV, an action potential is created and voltage gated sodium ion channels open causing sodium ions to rush into the cell in an event called depolarization. When the potential across the membrane has reached approximately $+30$ mV, voltage gated potassium channels open allowing potassium ions to leave the neuron and bring the potential across the membrane back down in an event called repolarization. This can result in a more negative potential than at rest, a state called hyperpolarization. The neuron is then in a refractory period during which it returns to -70 mV and cannot transmit information. The depolarization and repolarization of the membrane occurs in a highly localized fashion, creating an electrical impulse which propagates sensory information down the axon to the terminal (Biga et al., 2019).

Propagation of sensory information between neurons is mediated by molecules called neurotransmitters. When an action potential arrives at the axon terminal, calcium voltage gated ion channels are opened to increase the concentration of free intracellular calcium ions in the axon terminal of the neuron. Calcium is a necessary signaling ion for fast exocytosis of vesicles into the synapse (Südhof, 2012). First, vesicles of neurotransmitters are bound to the axonal membrane of the neuron by SNARE complexes composed of synaptobrevin, syntaxin 1 and SNAP-25. Once Ca^{2+} invades the axonal terminal, it binds to synaptotagmin 1 and causes the exocytosis of the vesicles already primed by the SNARE protein complex (Tang et al., 2006).

A synapse is a juncture between two communicating neurons. Neurotransmitters diffuse across the synapse to primarily interact with receptors on the surface of the receiving neuron. Neurotransmitters are cleared from the synapse by diffusion, enzyme catalyzed degradation, reuptake by the sending neuron via a transporter, or the neurotransmitters can bind to receptors

on the presynaptic terminal in a negative feedback inhibition loop. Many receptor proteins are G coupled protein receptors which are trans membrane proteins allowing for the extra cellular environment to impact cell signaling a secondary messenger cascades inside the cell.

2.3 Dopamine Synthesis and Signaling Pathways

Dopamine is synthesized from the amino acid L-tyrosine in a two-step reaction. The first step is rate limiting and catalyzed by the iron dependent enzyme tyrosine hydroxylase (TH) (Figure 1) (Ramsey et al., 1996)(Hillas & Fitzpatrick, 1996). Tyrosine hydroxylase is activated by cAMP dependent phosphokinase A and Ca^{2+} calmodulin dependent protein kinase II (Fujisawa & Okuno, 2005). Once synthesized, dopamine is then packaged into vesicles by a protein called vesicular monoamine transporter (VMAT). Vesicles are labeled as one of three distinct pools: readily releasable, recycle, and reserve pool (Denker & Rizzoli, 2010). Readily releasable vesicles are deployed immediately in response to stimulus, recycled vesicles are filled with dopamine that has been transported back into the neuron after released into the synapse. The reserve dopamine pool is rarely used but accounts for ~80-90% of dopamine molecules in a neuron (Ortiz et al., 2010).

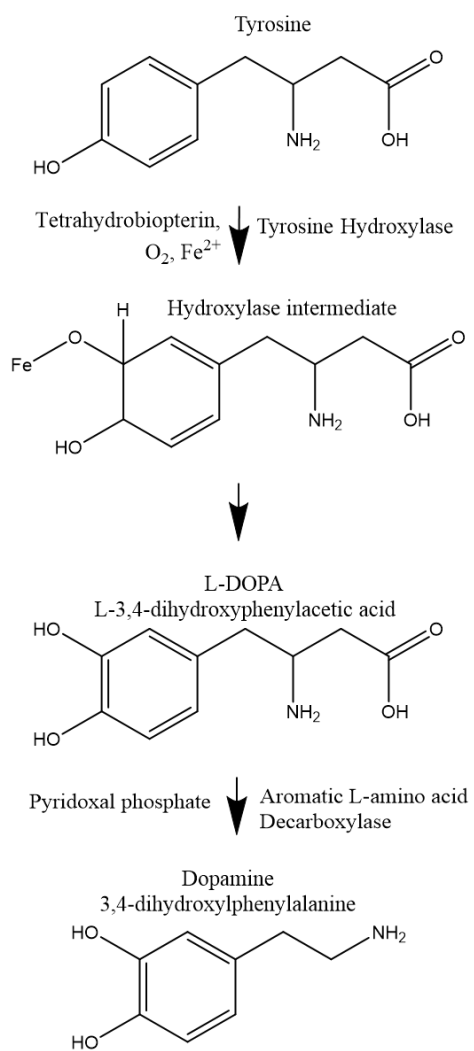


Figure 1. Dopamine synthesis pathway

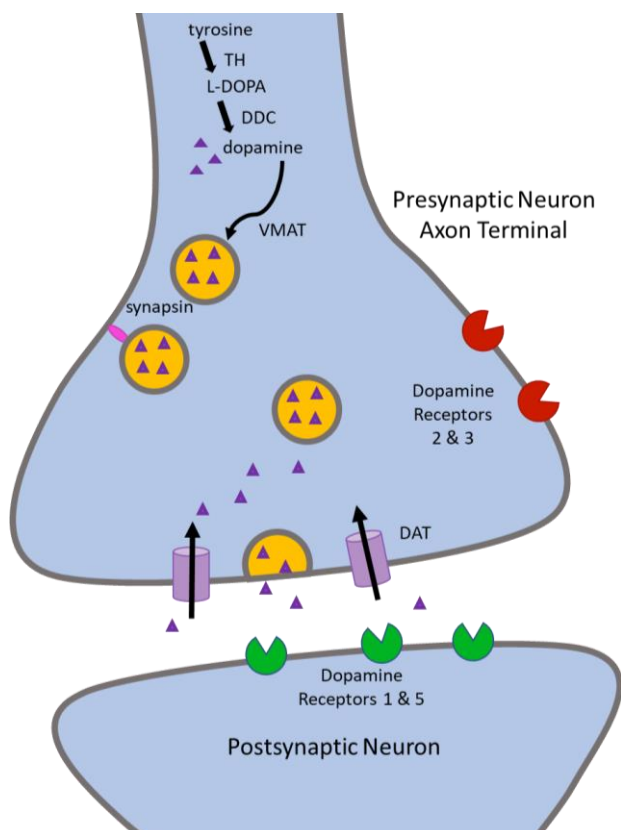


Figure 2. Cartoon of dopamine release in synapse showing vesicles, exocytosis, recycling and target protein interaction at the post synaptic terminal.

When an action potential reaches an axon terminal of dopaminergic neuron during neurotransmission, dopamine is released into the synapse and interacts with specific receptor proteins (Figure 2). There are five known target proteins identified as dopamine G coupled protein receptors labeled D1 to D5. Receptors D1 and D5 are classified as D1-like and are localized at the post synaptic terminal. Activation of these receptors propagates neurotransmission by upregulating cyclic adenosine monophosphate (cAMP) and several phosphokinases. Receptors D2, D3, and D4 are classified as D2- like receptors. These receptors are predominantly, localized at both the presynaptic and post synaptic terminals. Activation of these receptors decreases neurotransmission by down regulating cAMP and phosphokinases.

In addition, dopamine receptors can act on Ca^{2+} ion channels. Temporarily, the $G_{\beta\gamma}$ subunit of dopamine receptors can bind directly to voltage gated Ca^{2+} ion channels inhibiting ion exchange. More permanently, $G_{\alpha i}$ acts on second messenger cascades to decrease expression of voltage gated Ca^{2+} channels (Mishra et al., 2018). Without Ca^{2+} exchange, neurotransmitter vesicles cannot be released (Dong et al., 2018). G coupled protein receptors can be inhibited by zinc (Doboszewska et al., 2017).

To terminate the neurotransmission, dopamine transporter (DAT) transports dopamine in the synapse back into the presynaptic terminal where it is recycled. Alternatively, dopamine can also be cleared from the synapse by enzymatic degradation into metabolites. If the concentration of synaptic dopamine is sufficiently high, it can diffuse out of the synapse into extracellular space and interact with D2 and D3 receptors located on the presynaptic terminal (referred to as autoreceptors). These autoreceptors then inhibit dopamine synthesis and release in a feedback inhibition loop (Beaulieu & Gainetdinov, 2011).

Dopamine neurons in the midbrain are involved in distinct neuronal pathways (Figure 3). The mesolimbic and mesocortical pathways originate in the ventral tegmental area, projecting to the nucleus accumbens and frontal cortex, respectively. The mesolimbic pathway controls incentive salience and is the focus of addiction studies. The mesocortical pathway is implicated in learning and emotional responses and its dysfunction has been linked to disorders including schizophrenia. The nigrostriatal pathway originates in the substantia nigra and projects to the dorsal striatum. The nigrostriatal pathway controls movement and its dysfunction has been associated with Parkinson's disease. Lastly, the tuberoinfundibular pathway projects from the hypothalamus to the pituitary and dysfunction can produce abnormal lactation or menstrual disruptions (Puig et al., 2014) (Barron et al., 2010).

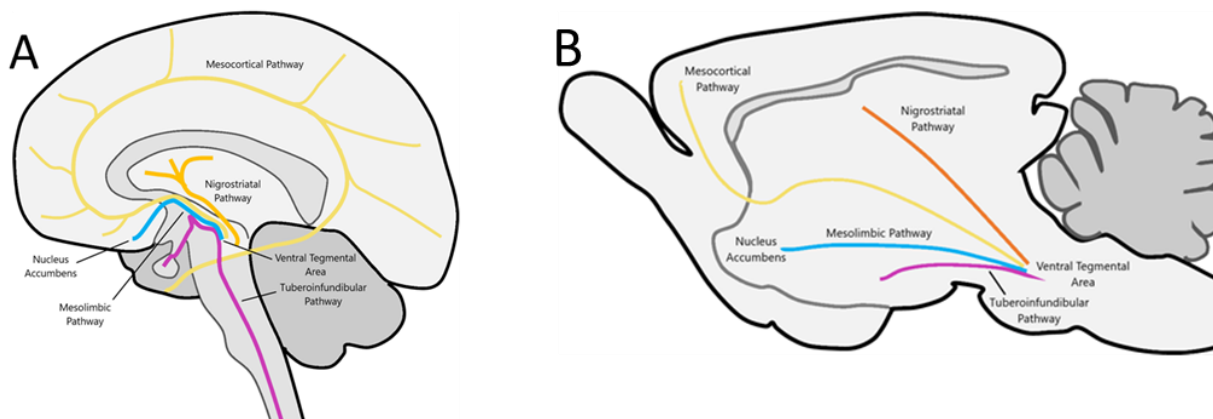


Figure 3. Dopaminergic pathways in the A) human and B) rodent brain. The pathways shown are tuberoinfundibular (pink), mesolimbic (blue), mesocortical (yellow), and nigrostriatal (orange.)

2.4 Neural Basis of Addiction

The mesolimbic pathway of the brain connects the ventral tegmental area containing the neurotransmitters dopamine, gamma-aminobutyric acid, and glutamic acid (Pierce & Kumaresan, 2006) to the nucleus accumbens. The mesolimbic pathway is predominantly dopaminergic, governs memory, addiction, and reward related behaviors (Adinoff, 2004), and is affected by drugs of abuse (Volkow et al., 2009). Typically, drugs of abuse increase extracellular dopamine release in the nucleus accumbens, but their mechanism of action may differ. For example, methamphetamine translocates DAT, which is a transmembrane pore, into a reverse orientation (Goodwin et al., 2009). Thus, dopamine in the cytosol is effluxed into the synapse instead of recycled into the neuron. However, Cocaine blocks DAT resulting in an increase in extracellular levels of dopamine (National Institute on Drug Abuse, 2016). In addition, it has been shown that acute cocaine administration inhibits synapsin. Synapsin is a protein responsible for anchoring reserve pool vesicles to the plasma membrane of a neuron, thus preventing dopamine release (Venton et al., 2006).

Clinical observations of individuals dealing with drug addiction reveal differences in brain physiology compared to individuals who have never experienced illicit drugs. Furthermore, Positron Emission Tomography (PET) scans have shown that individuals who used methamphetamine, cocaine, heroin, or abused alcohol have fewer available D2 receptors than individuals who have never abused those drugs (Volkow et al., 2009). The appearance of fewer available D2 receptors in PET scans is caused by the radiotracer failing to bind to D2 receptors. Radiotracers used in PET scans can be out competed in their binding site to D2 by endogenous dopamine. Therefore, the findings of fewer D2 receptors present can be explained by either an increase in dopamine or a decrease in the number of functional receptors (Volkow et al., 2009).

D2 receptors are further implicated in addiction by addiction vulnerability studies. Humans who would describe the administration of the stimulant methylphenidate (Ritalin) as pleasant had significantly fewer D2 receptors than those who described it as unpleasant (Volkow et al., 1999). In rats allowed to self-administer ethanol, inducing over expression of D2 receptors reduced the preference of individuals for ethanol as well as ethanol intake (Thanos et al., 2001). Macaques have also been examined, with individuals possessing a greater number of D2 receptors showing resilience to cocaine reinforcement training (Morgan et al., 2002).

Toluene inhalation has been shown to affect dopamine release in the nucleus accumbens (Apawu et al., 2015). While the definitive mode of action is yet to be elucidated, it is known that toluene inhibits N-methyl-D-aspartate (NMDA) glutamate activated ion channels which affect the excitability of neurons (Cruz et al., 2014). It is also known that cAMP, regulated in part by both classes of dopamine receptors, can modulate the transcription of genes through interaction with cAMP response element (CRE) transcription factor (Robison & Nestler, 2011). Identification of specific genes and whether CRE increases or decreases transcription is still

ongoing. Activation of this transcription response pathway resulting from frequent phasic dopamine release is thought to function as a coping or neuroprotective mechanism and result in tolerance to previously salient stimuli. While it is hypothesized that chronic toluene use ultimately results in a change in receptor expression, it has yet to be shown (Bowen et al., 2006).

Recent work has showed that acute (30 minute) inhalation of physiologically relevant doses of toluene (2000 and 4000 ppm) increases dopamine release in the nucleus accumbens and caudate putamen of adult male Swiss Webster mice (Apawu et al., 2015). However, modeling chronic use with repeated exposure over seven consecutive days at these same doses leads to attenuation of dopamine release exclusively in the nucleus accumbens (Apawu et al., 2015). From these findings, it can be hypothesized that the decrease in dopamine release following chronic toluene inhalation is the result of a compensatory effect. This compensatory effect may be mediated by dopamine autoreceptors D2 and D3 in a feedback inhibition mechanism. D2 receptors have been widely implicated in the action of most drugs of abuse, whereas there is little to no known involvement of the D3 receptors (Le Foll et al., 2005).

2.5 Fast Scan Cyclic Voltammetry

Fast Scan Cyclic Voltammetry (FSCV) is an analytical technique used to monitor electroactive biomolecules. FSCV is particularly useful for the study of neurotransmission because it can capture the fast neural process on a millisecond timescale, quantifying the release and uptake of neurotransmitters in a nanomolar range. The technique uses a working electrode, usually carbon fiber microelectrode, which is inert and causes minimal trauma to brain tissue (Roberts & Sombers, 2018). FSCV works applying an electrical potential in a triangular waveform (Figure 4A) across the working electrode surface relative to a reference electrode, typically, a silver-silver electrode. The redox reaction of the analyte leads to current that is recorded and related to the analyte concentration. In slice or anaesthetized subjects, a stimulating

electrode is commonly used to elicit neurotransmitter release via electrical stimulation. More recently optogenetics have been developed where neurons are genetically modified to express opsin proteins, such as Channelrhodopsin-2, which react to light (Nagel et al., 2005). These neurons can be stimulated with light by a fiber optic cable in either anesthetized animals or brain slices. Neurotransmitter release in optogenetic studies can be monitored with electrophysiology, voltage sensitive dyes, or functional magnetic resonance imaging (Lim et al., 2013).

The data generated from FSCV can be displayed as a voltammogram which is a current versus voltage plot (Figure 4B), a current versus time trace (not shown) and a 3-D pseudo color plot (Figure 4C) where the x axis is time, the y axis is potential, and the color in the plane, green and blue represent oxidation and reduction currents respectively.

While FSCV can be used to analyze neurotransmitters in anesthetized and free behaving animals, the slice method offers an additional level of control with pharmaceutical manipulations, that can happen quickly with minimal washout time. In addition, placement of electrodes is more consistent when using *slice* FSCV because the investigator can see brain structures with the naked eye without relying on stereotaxic coordinates. Slice FSCV relies on preserving brain viability postmortem. To accomplish this, the brain slices are kept in a chamber that continually circulates warm, oxygenated artificial cerebral spinal fluid (aCSF) with glucose at physiological pH (pH 7.4) (Figure 5).

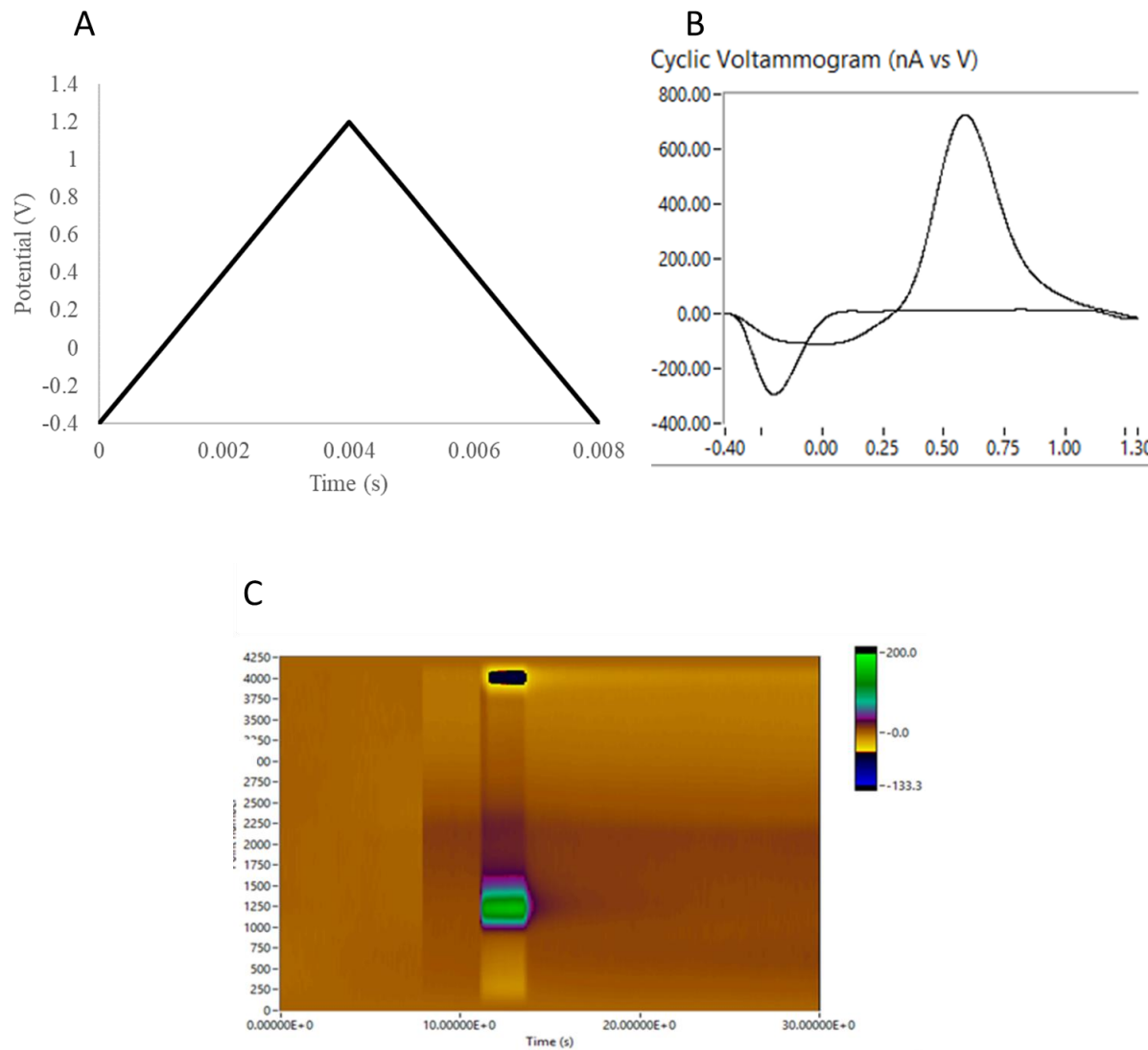


Figure 4. Fast scan cyclic voltammetry. (A) Applied waveform (B) Cyclic voltammogram (C) 3-D pseudo color plot.

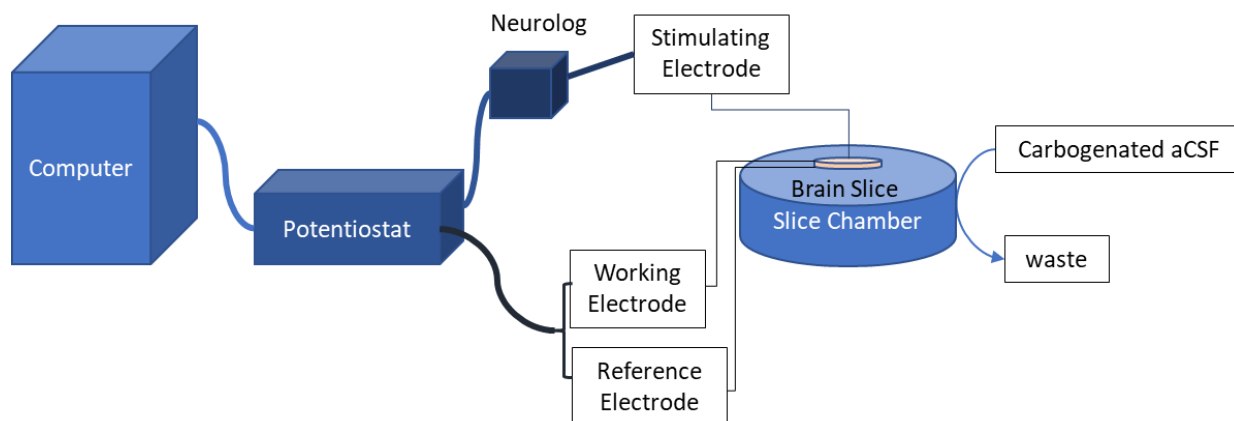


Figure 5. Schematic of slice FSCV. The potentiostat both controls brain stimulation through the neurolog device as well as records the evoked response through the working and reference electrodes. The brain slice is kept viable by mimicking conditions in intact brain. Brain slices are constantly perfused with warm oxygenated aCSF.

2.6 X-Ray Fluorescence (XRF) Spectrometry

X-ray fluorescence (XRF) spectrometry works by irradiating a sample with a high energy laser to ionize an electron from K or L energy levels. The ejected electron is replaced by an electron from a higher energy level, which emits a photon in the process. The photon emitted is in the x-ray region and its wavelength is characteristic of the element the electron was associated with (Figure 6). The intensity of energy measured by the detector is proportional to the abundance of each element in the sample. X-ray fluorescence spectrometry can be used quantitatively if a standard of known concentration is added to samples prior to analysis (Wirth & Barth, 2020).

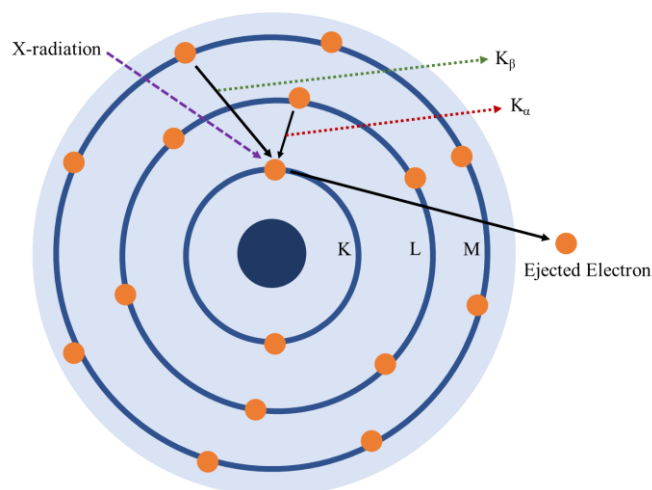


Figure 6. Schematic of showing the principles behind X-ray fluorescence spectrometry. Incident radiation ejects an electron in an inner shell of an atom. Outer electrons fill the hole and fluoresce a photon to lose the appropriate energy.

XRF instruments use a high energy laser to generate x-rays in combination with a monochromator to irradiate samples at a very shallow incident angle. Most of the incident x-ray is not focused into the detector (Figure 7).

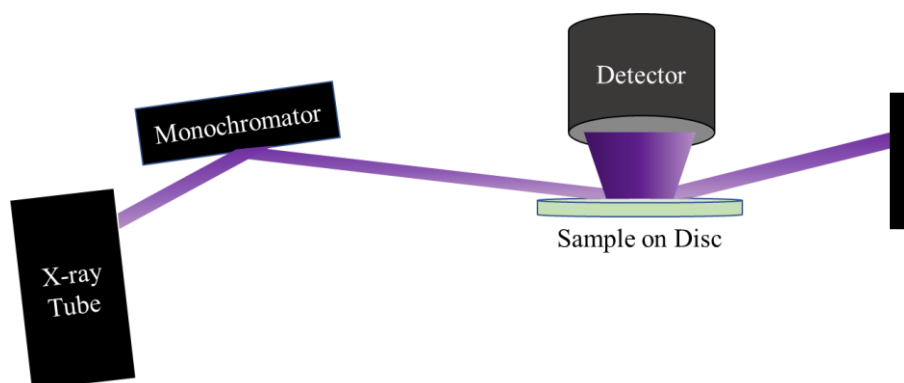


Figure 7. Schematic of XRF Instrumentation. X-Rays are produced from a high voltage laser. A monochromator is used to select a narrow range of suitable wavelengths before reflecting radiation on to the sample. Most of the x-radiation continues past the sample and only a fraction is detected.

CHAPTER 3

METHODOLOGY

3.1 Toluene Exposure Paradigm

A total of 63 adult male and female Swiss Webster mice (10-12 weeks, 25-30 grams) were used to maintain consistency with previously reported work. All animal procedures were carried out in accordance to *the Guideline for the Care and Use of Laboratory Animals* as approved by the University of Northern Colorado's Institutional Animal Care and Use Committee (IACUC). The mice were divided into three experimental groups; i) air control ii) 2000 ppm toluene exposed and iii) 4000 ppm toluene exposed groups. The period of toluene exposure was 30 minutes each day for seven consecutive days. On the seventh day, brain tissues from the nucleus accumbens of these mice were harvested for fast scan cyclic voltammetry, immunocytochemistry, or XRF analysis (Figure 8).

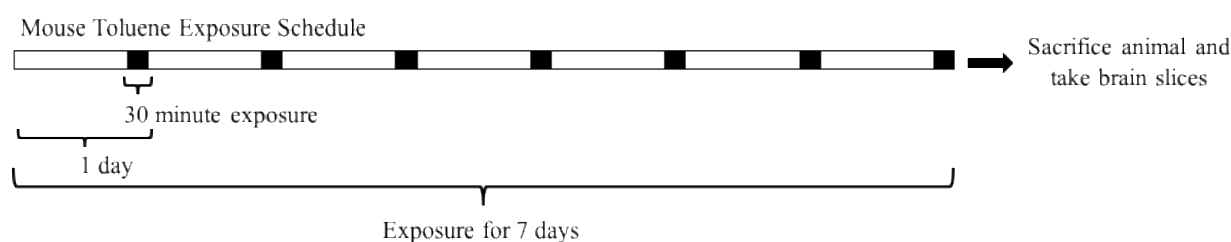


Figure 8. Chronic Toluene exposure protocol.

Mice were exposed in a 26.5 liter pyrex glass jar with a lid. On the lid is mounted a port (Figure 9A) through which toluene was injected onto filter paper (Figure 9B). A fan directly above the filter paper circulated air in the chamber and helped to quickly evaporate the toluene. Additionally, on the lid there is a port and hose through which to take gas samples (Figure 9C).

During exposures animals could freely roam in the bottom of the sealed exposure chamber, approximately 50 cm away from the fan.

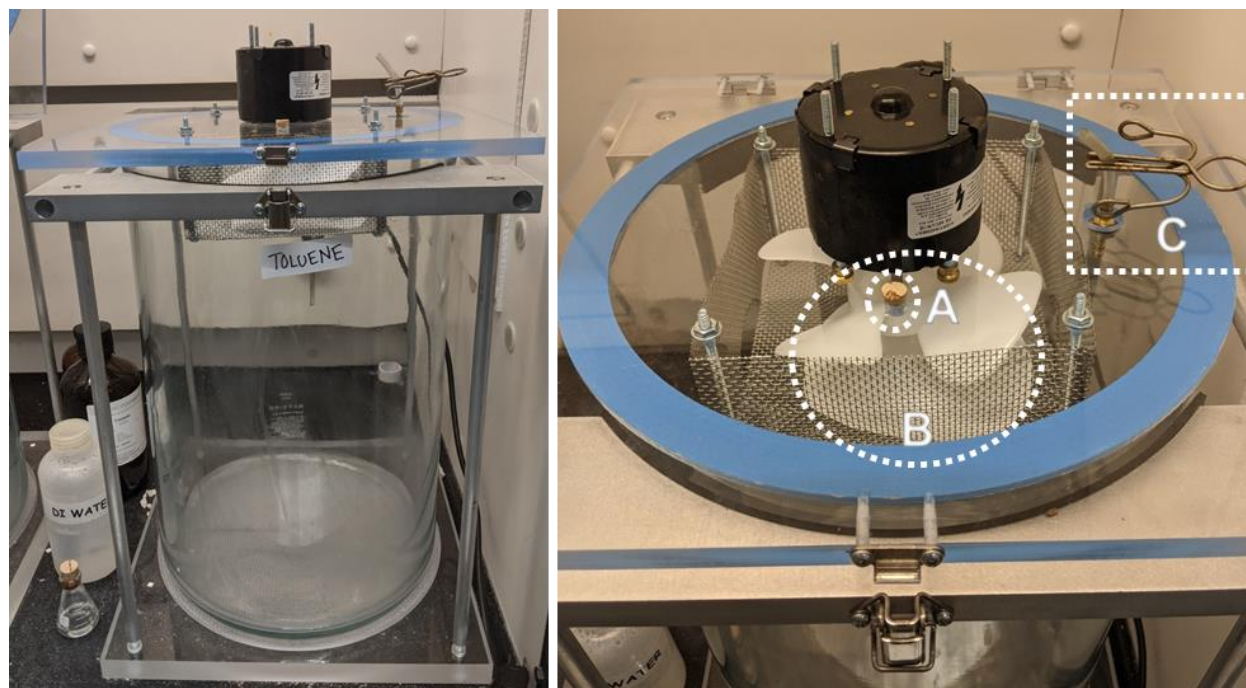


Figure 9. Toluene exposure chamber constructed from a 26.5 L Pyrex jar (left) and fitted with an air-tight lid (right.) Toluene is introduced to the sealed chamber through the port (A) and dispensed onto filter paper in front of a fan (B) to expedite evaporation and circulation. Gas samples for FTIR were taken from (C). The entire exposure chamber is housed in a fume hood.

Appropriate dosing of the chamber was calculated using the ideal gas law (equation 1).

Notably, this research takes place at 1,425 meters above sea level where the ambient pressure averages 0.8500 atmospheres. 2000 ppm of toluene gas was calculated as equivalent to 0.1965 mL of liquid toluene (equation 3).

$$n = \frac{0.8500 \text{ atm} \cdot 26.5 \text{ L}}{0.0821 \text{ L atm mol}^{-1} \text{K}^{-1} \cdot 296.7 \text{ K}} = 0.9247 \text{ moles} \quad \text{eq. 1}$$

$$0.9247 \cdot (2 \cdot 10^{-3}) = 1.849 \cdot 10^{-3} \text{ moles} \quad \text{eq. 2}$$

$$1.849 \cdot 10^{-3} \text{ moles} \cdot \frac{92.14 \text{ grams}}{\text{mole}} \cdot \frac{\text{mililiter}}{0.867 \text{ grams}} = 0.1965 \text{ mL Toluene} \quad \text{eq. 3}$$

3.2 Verification of Toluene Concentration in the Chamber Using Fourier Transform Infrared Spectroscopy

To verify the concentration of toluene in the exposure chamber, an appropriate volume of toluene was aliquoted into the chamber and the fan turned on. After ten minutes a 10 cm pathlength gas cell was filled with a sample of the chamber atmosphere. Using Fourier Transform Infrared Spectroscopy (FTIR), the absorbance of the gas cell at 729 cm^{-1} ($13,717\text{ nm}$) was used to create a Beer's plot. A peak at 729 cm^{-1} represents the out of plane bending of carbon-hydrogen bonds on the aromatic ring of toluene.

3.3 Slice Fast Scan Cyclic Voltammetry (FSCV) Measurement of Dopamine Release in the Nucleus Accumbens

Harvested brains from toluene-exposed or air control mice were sectioned into $400\text{ }\mu\text{m}$ coronal slices such that nucleus accumbens was exposed. The slices were kept viable in oxygenated artificial cerebrospinal fluid (aCSF) under physiological temperature and pH.

A carbon fiber working electrode and a tungsten stimulating electrode were positioned $100 - 200\text{ }\mu\text{m}$ away from each other on a brain slice placed in a recording chamber (Figure 10). Dopamine release was electrically evoked by the stimulating electrode and an electrical potential was applied at the working electrode surface using a triangular wave form from -0.4 V to $+0.2\text{ V}$ and back to -0.4 V with respect to a Ag/AgCl reference electrode at a scan rate of 400 V/s . The stimulated dopamine was oxidized into dopamine-o-quinone during the forward scan, whereas in the reverse scan, dopamine-o-quinone was reduced back to dopamine. The current generated as a result of the redox reaction was measured by the working electrode and reported as a concentration of dopamine (Figure 10).

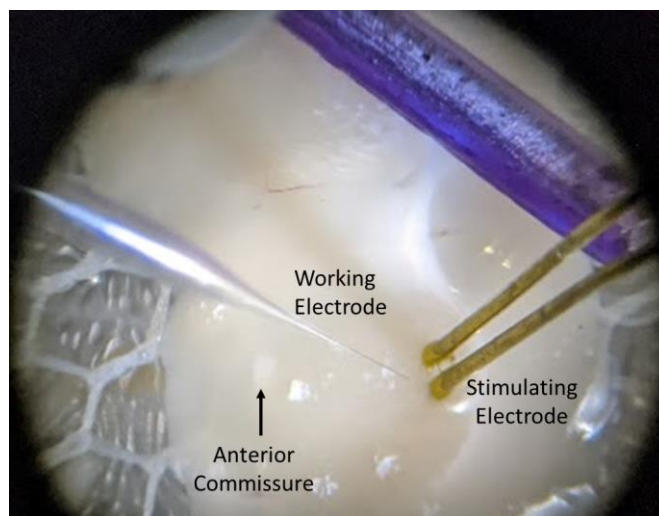


Figure 10. Electrode placement for slice FSCV. The working electrode has 50 μm of exposed carbon fiber which is inserted into the brain slice approximately 150 μm from the two pronged stimulating electrode.

3.4 Measurement of Dopamine D2 Receptor Distribution Using Immunocytochemistry

Immunocytochemistry allows the dopamine receptor distribution to be visualized. The distribution of dopamine D2 receptors in the nucleus accumbens was examined in 30 μm thick coronal brain sections between bregma +1.10 and +1.18. Slices in this region were identified by the physiology of the corpus collosum. Slices were fixed in 2% paraformaldehyde in ethanol. Slices (air control $n=10$, 2000 ppm $n=10$, 4000 ppm $n=10$) were labeled for dopamine receptor D2 by incubating with 1:1000 polyclonal extra cellular rabbit anti mouse D2 antibody (Alomone Labs Ltd., Jerusalem, Israel) for 48 hours at 4 °C. Brain sections were incubated with 1:5000 goat anti rabbit Alexfluor-488 secondary antibody (Jackson Immuno Research Laboratories, West Gove, PA, USA) for 2 hours at room temperature, washed, cover slipped and imaged with a Zeiss confocal microscope with a 20x objective and 2x digital zoom (40x total.)

3.5 X-Ray Fluorescence Spectrometric Measurements of Metals in Brain Tissues

Tissue from the nucleus accumbens (air control $n = 10$, 4000 ppm exposed $n = 10$) was analyzed. The nucleus accumbens was harvested from animals postmortem by using a matrix to take a 2 millimeter coronal slice at approximately +2.0 mm from bregma. Then a 1-millimeter diameter biopsy punch was used to remove tissue immediately ventral to the anterior commissure. Tissue from right and left hemispheres were combined, lysed in 19 μL 0.5% mass per volume nitric acid and homogenized by sonication. A 1 μL 20 ppm internal gallium standard was added to each sample resulting in a final volume of 20 μL with a concentration of 1 ppm Ga. An aliquot of 10 μL was dotted onto an acrylic disc, allowed to dry in the oven at 105° C, and analyzed via XRF for potassium, calcium, iron, copper, and zinc.

3.6 Data Analyses

3.6.1 Analysis of Fast Scan Cyclic Voltammetry Data

To determine the impact of chronic toluene exposure on evoked dopamine release, the baseline signals, i.e. stable signals evoked from air control and 4000 ppm toluene exposed mice were converted into molarity of dopamine and compared.

The magnitude of dopamine evoked from brain slices was extracted from FSCV recordings by creating a training set in HDCV Analysis v1001 software (University of North Carolina). An HDCV training set used flow cell data to correlate the magnitude of current to molarity of dopamine present (amps to molarity conversion factor) and created an average voltammogram (K matrix) to locate in recordings. Flow cells were constructed of a 30 mL syringe of glucose free aCSF which flowed through a T-junction at 1 mL per minute and 12 mL syringe of 500 nM dopamine which was injected into the same t junction in 1 mL aliquots 5 seconds after flow cell recordings began.

Training sets were constructed from at least four flow cell runs per electrode. Peak currents were identified by the software at any potential. If the current showed a 0.1 second spike before a plateau, the plateau value was used for peak current. Concentrations were captured at data point 450 which correlates to a potential of +1 V where the cyclic voltammograms had a peak or valley with a high degree of homology. The training set was used to produce time vs concentration plots of dopamine from slice FSCV recordings. The dopamine evoked was calculated as the change in concentration spike over 0.1 seconds immediately after stimulation.

Baseline evoked dopamine was calculated per individual as the average of 6 recordings spaced 5 minutes apart. Average baseline signals were graphed and a one-way ANOVA ($\alpha = 0.05$) was performed using GraphPad Prism Software.

3.6.2 Analysis of Immunocytochemistry Data

The nucleus accumbens was identified on microscopy images by its location immediately ventral to the anterior commissure fiber tract (Figure 11). The nucleus accumbens was further differentiated into a 300 x 600 μm rectangle around the core and a 300 x 300 μm square around the more medial and ventral shell. D2 receptors were identified and counted by ImageJ based on having a size larger than 4 square pixels and the highest 1% fluorescent intensity (Figure 12).

Receptor counts were normalized per 100 μm^2 area. Each condition, air control, 2000 ppm and 4000 ppm, contained 5 males and 5 females. If the results of a t test suggested no significant difference between the sexes in each condition, the counts were pooled in future analyses. A one way-ANOVA ($\alpha = 0.05$) was run to analyze D2 counts in the core and shell differentiated by exposure condition.

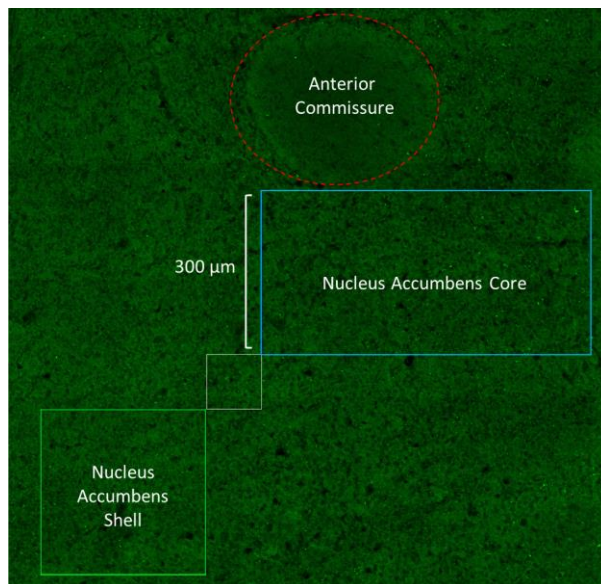


Figure 11. Identification of nucleus accumbens core and shell for ICC analysis.

3.6.3 Analysis of X-Ray Fluorescence Data

Spectral peaks from XRF analysis were auto identified by Bruker Picofox software, and concentration was reported in mg L^{-1} (ppm). Both air control and 4000 ppm toluene exposed groups contained 5 male and 5 female mice. Data was graphed and a one-way ANOVA ($\alpha = 0.05$) was performed using GraphPad Prism Software. If the results suggested no significant difference between the sexes in each condition, male and female results were pooled and the analysis re-run.

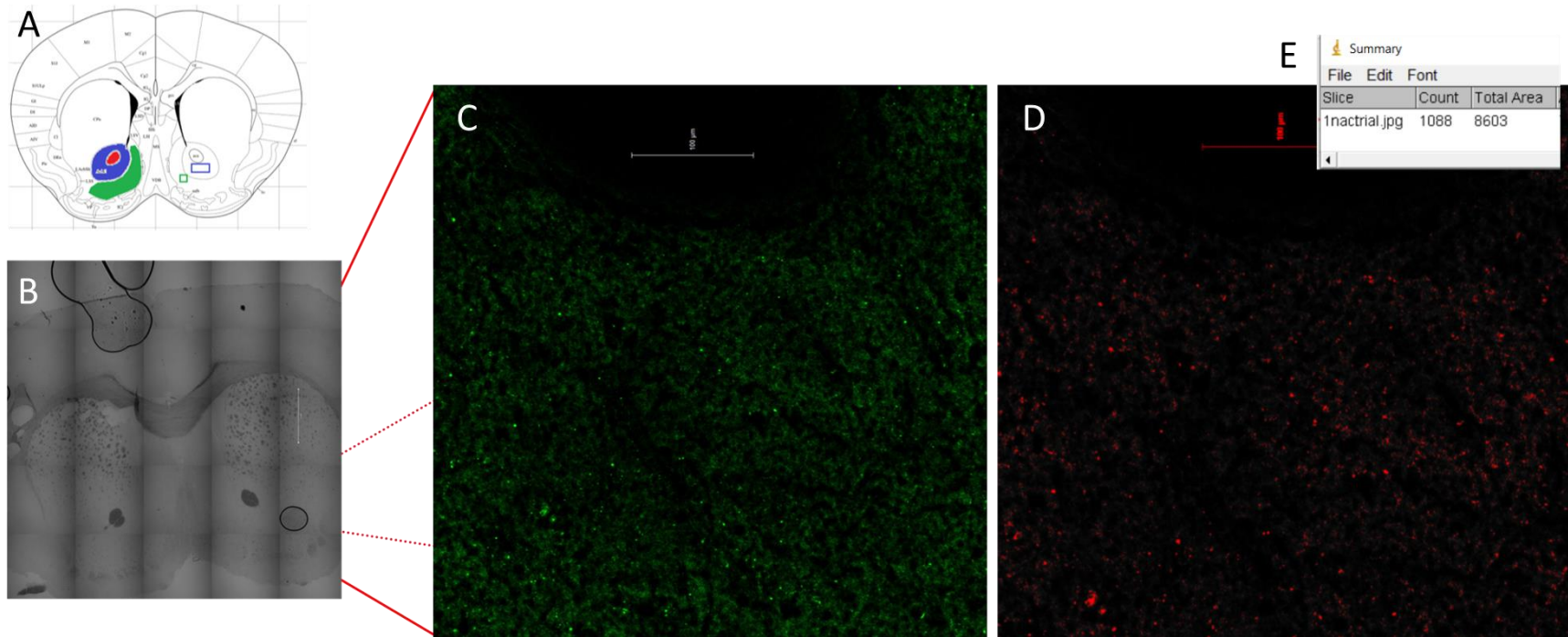


Figure 12. (A) Coronal section, bregma +1.18 mm, labeling anterior commissure in red, nucleus accumbens core in blue, and nucleus accumbens shell in green. (Paxinos & Franklin, 2001). (B) stitched image of transmitted light microscopy in coronal mouse slice (C) 40x image of Alexfluor-488 staining for D2 receptors in the nucleus accumbens (100 μm bar.) (D) Fluorescence counted as positive staining by ImageJ highlighted in red (E) Readout of receptor count from ImageJ.

CHAPTER 4

RESULTS

4.1 Verification of Toluene Concentration in the Exposure Chamber Using Fourier Transform Infrared Spectroscopy

To ensure animal subjects received consistent toluene exposure gas phase FTIR was used to analyze the chamber atmosphere. The absorbance intensity of spectral peaks at 728 cm^{-1} (Figure 13) were used to create a Beer's law plot (Figure 14). The infrared spectrum between 650 and 780 cm^{-1} showed the expected out of plane bending of C-H bonds on the aromatic ring of toluene. Because of the methyl substituent on the aromatic ring, not all hydrogens in toluene are equivalent and there is a secondary out of plane bending peak at 694 cm^{-1} . The Beer's law plot shows a linear correlation between toluene concentration and absorbance, as a simple linear regression had an R^2 value of 0.992. The extinction coefficient of toluene at 728 cm^{-1} was calculated to be $1.255 \times 10^{-5}\text{ cm}^{-1}\text{ ppm}^{-1}$.

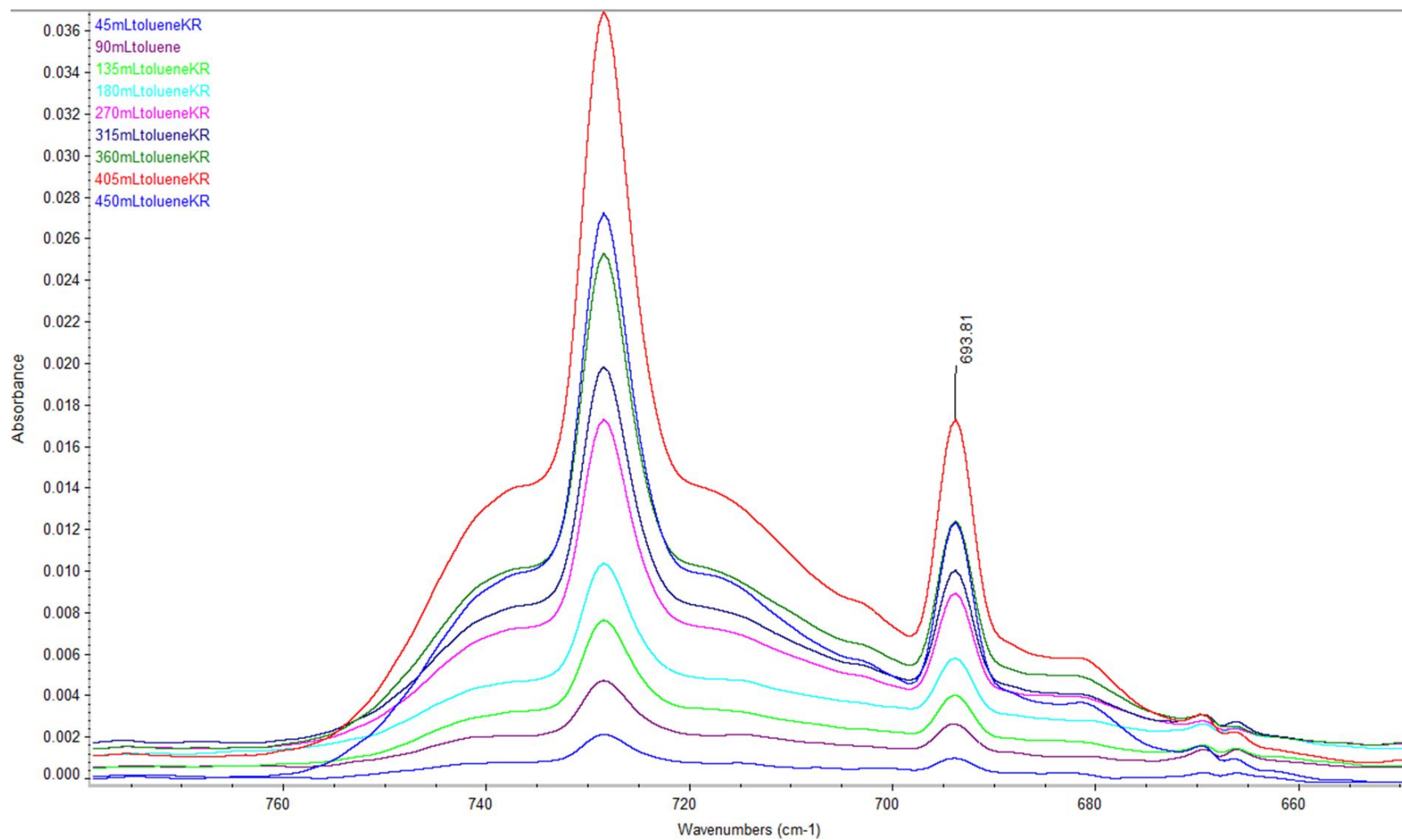


Figure 13. Infrared absorbance spectra of toluene in room air from 650-780 cm⁻¹.

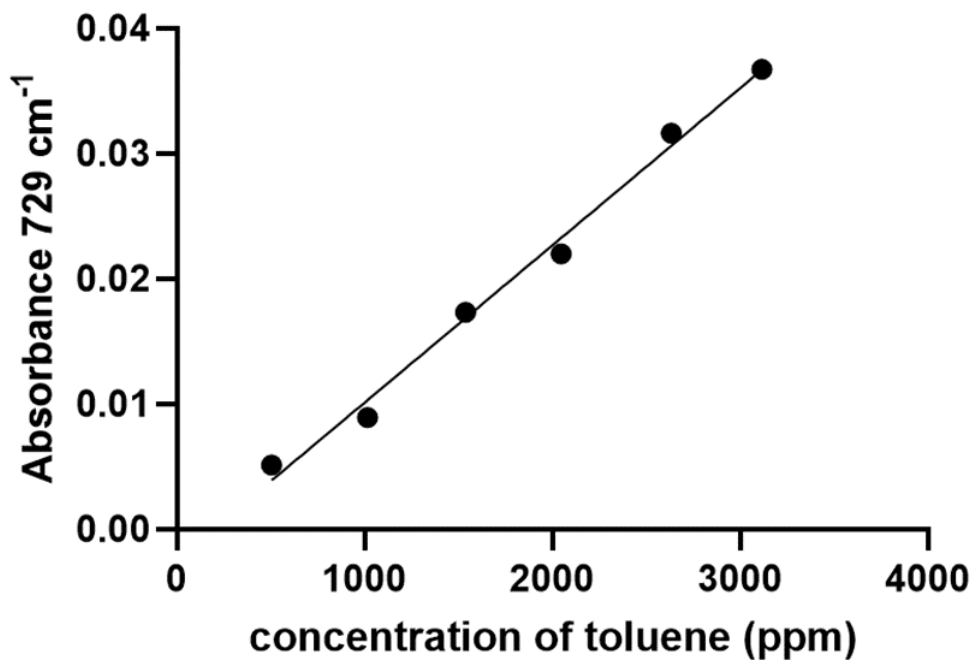


Figure 14. Beer's Law plot of toluene gas in room air. Extinction coefficient = $1.255 \text{ E-}5 \text{ cm}^{-1} \text{ ppm}^{-1}$, $R^2 = 0.992$, intercept = -0.00246 .

4.2 Slice Fast Scan Cyclic Voltammetry Measurement of Dopamine Release in the Nucleus Accumbens

This investigation confirmed the findings that chronic toluene exposure decreases dopamine release in the nucleus accumbens. The evoked dopamine baseline signals from air controls ($n = 8$; 4 male, 4 female) and 4000 ppm toluene exposed mice ($n = 5$; 3 male, 2 female) were compared using slice FSCV. When data from males and females are combined, control animals appeared to have evoked more dopamine, 204.7 nM, than toluene exposed animals, 42.43 nM, $t(11) = 2.041$, $p = 0.066$ (Figure 15A), but the difference is not statistically significant ($\alpha = 0.05$) due to variability between control males and females. When data from males and females are considered separately, control males released significantly ($p < 0.05$) more dopamine on average (344.8 nM) than from control females (76.53 nM); toluene exposed males (42.80 nM); or toluene exposed females, (41.60 nM, Figure 15B).

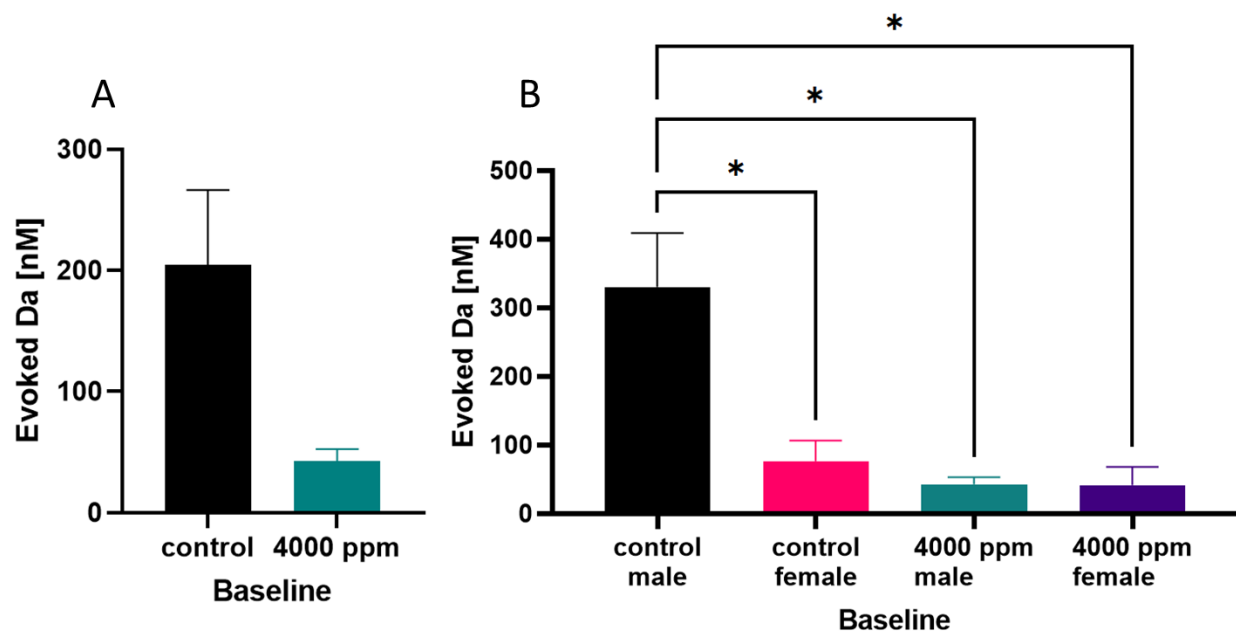


Figure 15. Evoked dopamine from control and exposed mice. (A) Male and female data combined reveal no significant difference between air control ($n=8$) and 4000 ppm toluene exposed mice ($n=5$). (B) Control male mice ($n=4$) released significantly more dopamine than any other group ($p<0.05$) but there was no significant difference between the other two groups. *denotes significance where $p = 0.05$.

4.3 Measurement of Dopamine D2 Receptor Distribution Using Immunocytochemistry

To investigate adaption to chronic toluene exposure and explore the role of D2 in possible compensation, the density of D2 receptors in the nucleus accumbens core and shell was mapped with immunocytochemistry. The nucleus accumbens core and shell were identified and imaged (Figure 16A and 16B). ImageJ was used to quantify receptor counts in these identified regions. Receptor counts were normalized for area prior to running a one-way ANOVA.

There were significantly more D2 receptors in the nucleus accumbens core (10.58 per $100 \mu\text{m}^2$) than the shell (4.89 per $100 \mu\text{m}^2$) for air control mice ($t(18) = 2.747$, $p 0.013$; Figure 17A). However, there was no significant difference in the average receptor counts in the toluene exposed group (Figure 17B, Table 1). Furthermore, there was no significant difference in receptor count between sexes in any of the experimental groups (Table 1).

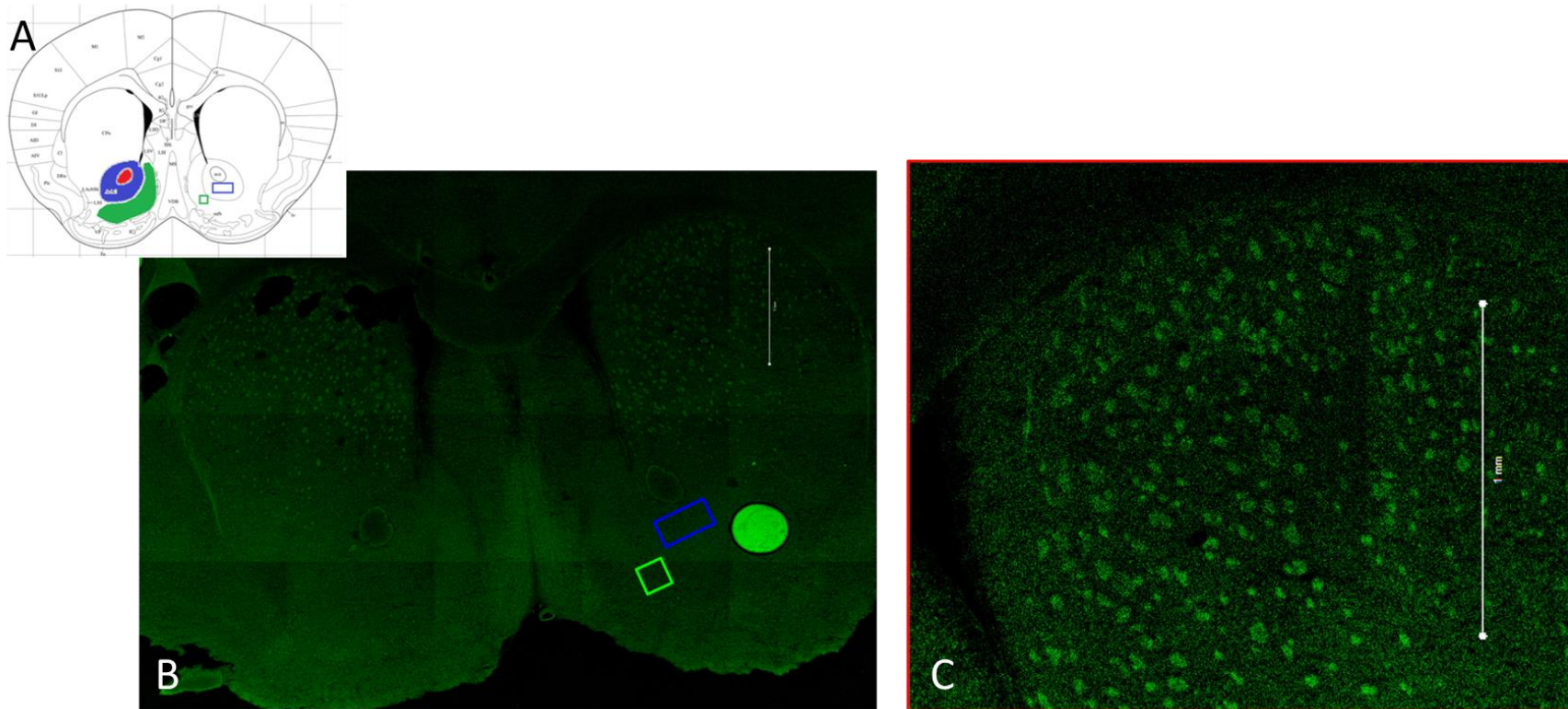


Figure 16. (A) Coronal section, bregma +1.18 mm, labeling anterior commissure in red, nucleus accumbens core in blue, and nucleus accumbens shell in green. (Paxinos & Franklin, 2001). (B) Stitched image of coronal slice stained for D2 and visualized with Alexafluor-488 (1 mm bar). Blue and green boxes indicate counting regions for the nucleus accumbens core and shell respectively and correspond to the boxes drawn in (A). (C) An enlargement of the caudate putamen (1 mm bar) showing positive staining in bright green punctation on top of background fluorescence.

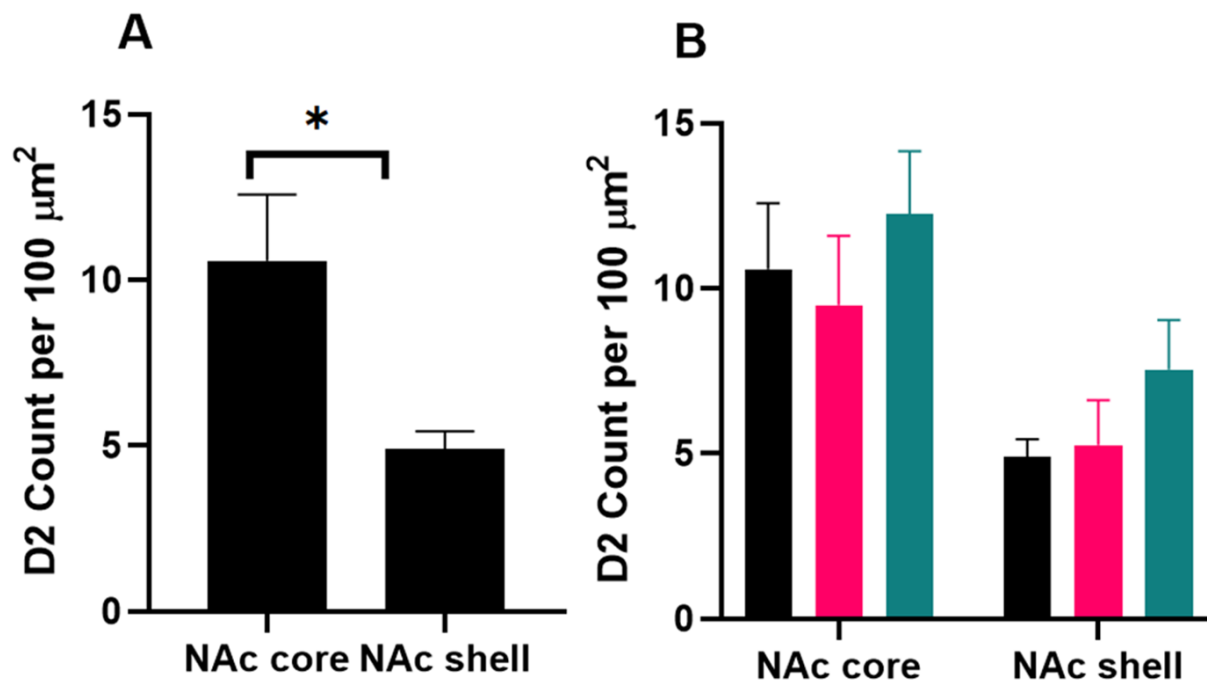


Figure 17. (A) The Nucleus Accumbens core ($M= 10.58$, $n=10$) had more D2 receptors per 100 μm^2 than the shell ($M=4.889$, $n=10$) for air control, $t(18)= 2.747$ $p= 0.0133$. (B) There was no significant difference in D2 receptors per 100 μm^2 within the same brain region based on treatment with air control (black), 2000 ppm (pink), or 4000 ppm (green) $F(2, 57)=3.857$, $p=0.268$. * denotes significance at $\alpha=0.05$.

Table 1. ANOVA results comparing D2 receptor counts per 100 μm^2 by brain region and treatment.

	Core	Shell
Air control	10.58	4.89
2000 ppm	9.49	5.26
4000 ppm	12.24	7.54
$F(2, 27)$	0.476	1.407
P	0.6265	0.2622

Table 2. t test for sex differences in the receptor analysis.

Treatment (male vs. females)	t(8)	P
Air	1.325	0.2219
2000	0.7635	0.4671
4000	0.5151	0.6204

4.4 X-Ray Fluorescence Spectrometric Measurements of Biometals in Brain Tissue

Cell signaling and response pathways are complex and frequently rely on ion cofactors. To further illuminate processes which may be affected by chronic toluene exposure, elemental analysis of nucleus accumbens biopsies was conducted by X-ray fluorescence.

Spectra were collected from control and toluene exposed animals (Figures 18 and 19). Both control and exposed animals showed only potassium, calcium, iron, copper, and zinc present between 3-11 keV. Note that the peak at 9.25 keV is the primary $K_{\alpha 1}$ emission from the 1 ppm gallium standard, the shorter peak at 10.26 keV is the $K_{\beta 1}$ emission from gallium, and the large peak after 15 keV is an artifact from the molybdenum laser in the instrument. Quantification was based off peak intensity relative to the gallium standard of known concentration, thus the shorter gallium peak in the spectra of toluene exposed animals is indicative of higher concentrations of the elements of interest (Figure 19).

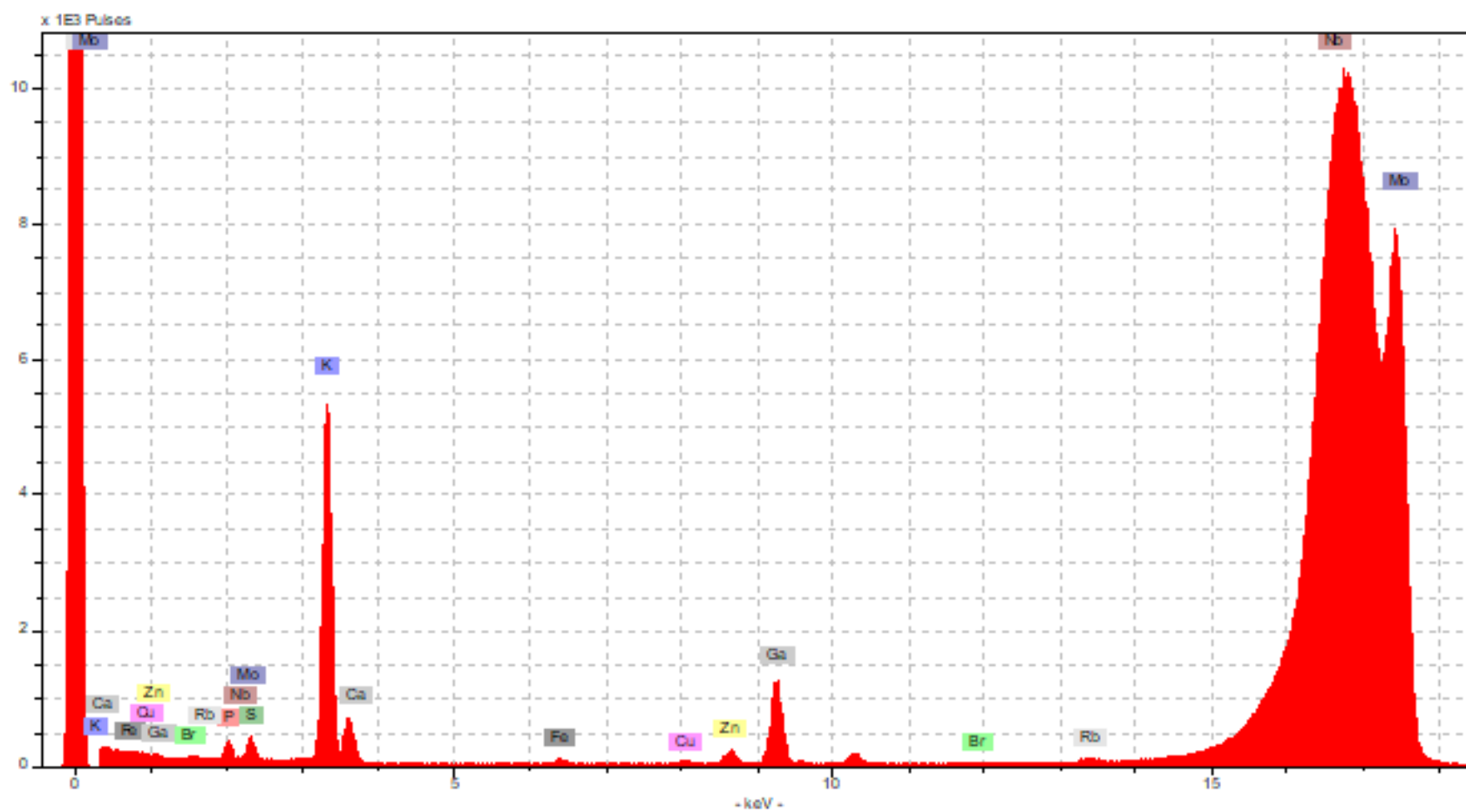


Figure 18. XRF spectra from a control animal using a Molybdenum laser source and internal 1 ppm Gallium standard.

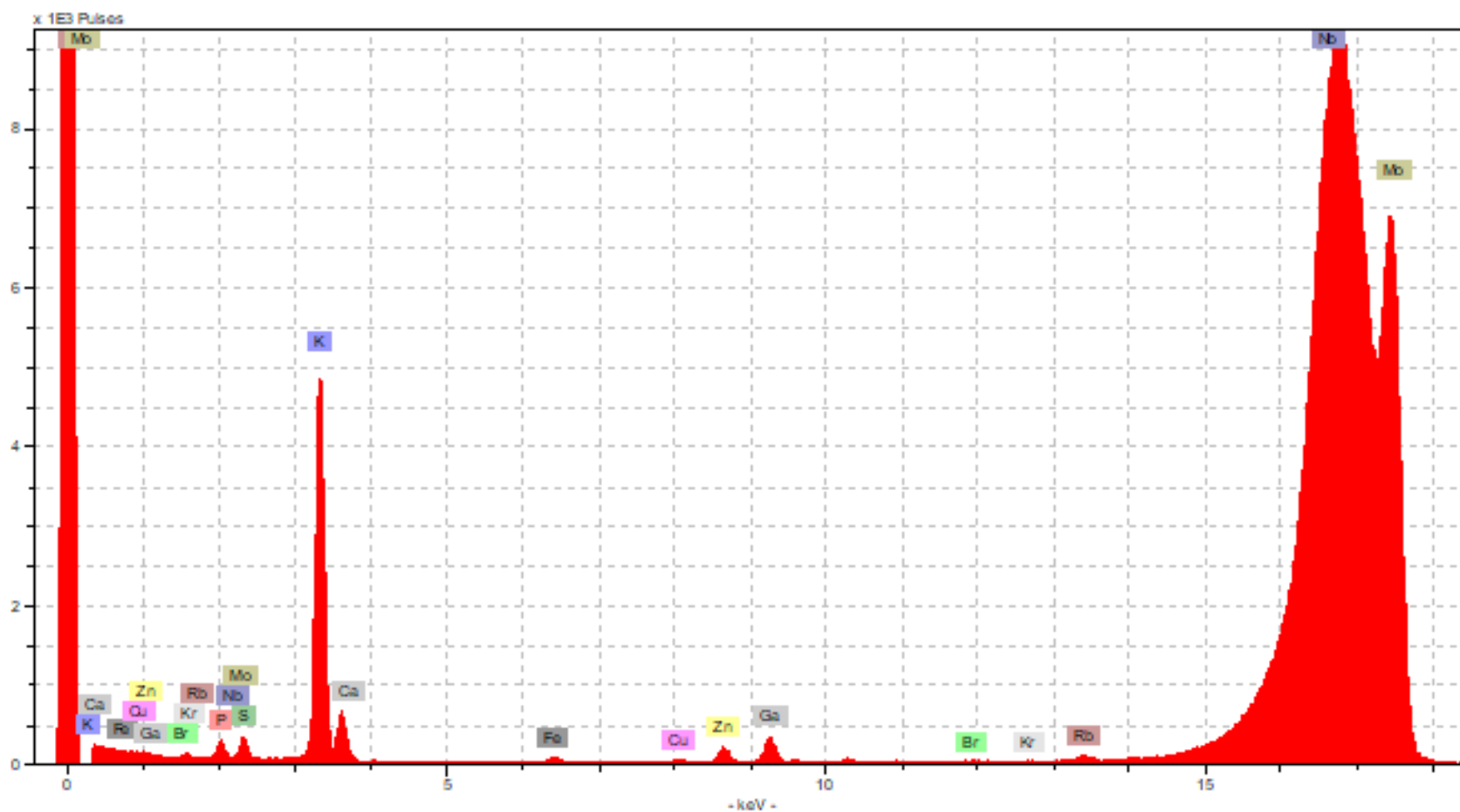


Figure 19. XRF spectra from an exposed animal using a Molybdenum laser source and internal 1 ppm Gallium standard.

Results were adjusted for the lysate dilution factor and mass of wet tissue lysed. There was no significant difference between sexes (Figure 20), therefore male and female results were pooled, and a two tail t test ($\alpha = 0.05$) was run to detect significance between control and toluene exposed mice (Table 3). On average, every metal analyzed appeared to have a higher concentration in toluene exposed animals (Figure 21). However, it was only iron that showed significant difference between the two experimental groups ($t(17) = 2.171, p = 0.044$).

Table 1 Concentration in ppm of elements determined by XRF where male and female data are pooled.

	Control ($\mu\text{g g}^{-1}$)	Toluene exposed ($\mu\text{g g}^{-1}$)	t (df)	<i>P</i>
K	1019	1379	1.186 (17)	0.252
Ca	15.39	24.64	1.897 (17)	0.075
Fe	2.218	3.613	2.171 (17)	0.044
Cu	1.013	1.271	0.891 (16)	0.386
Zn	4.590	5.696	0.913 (17)	0.374

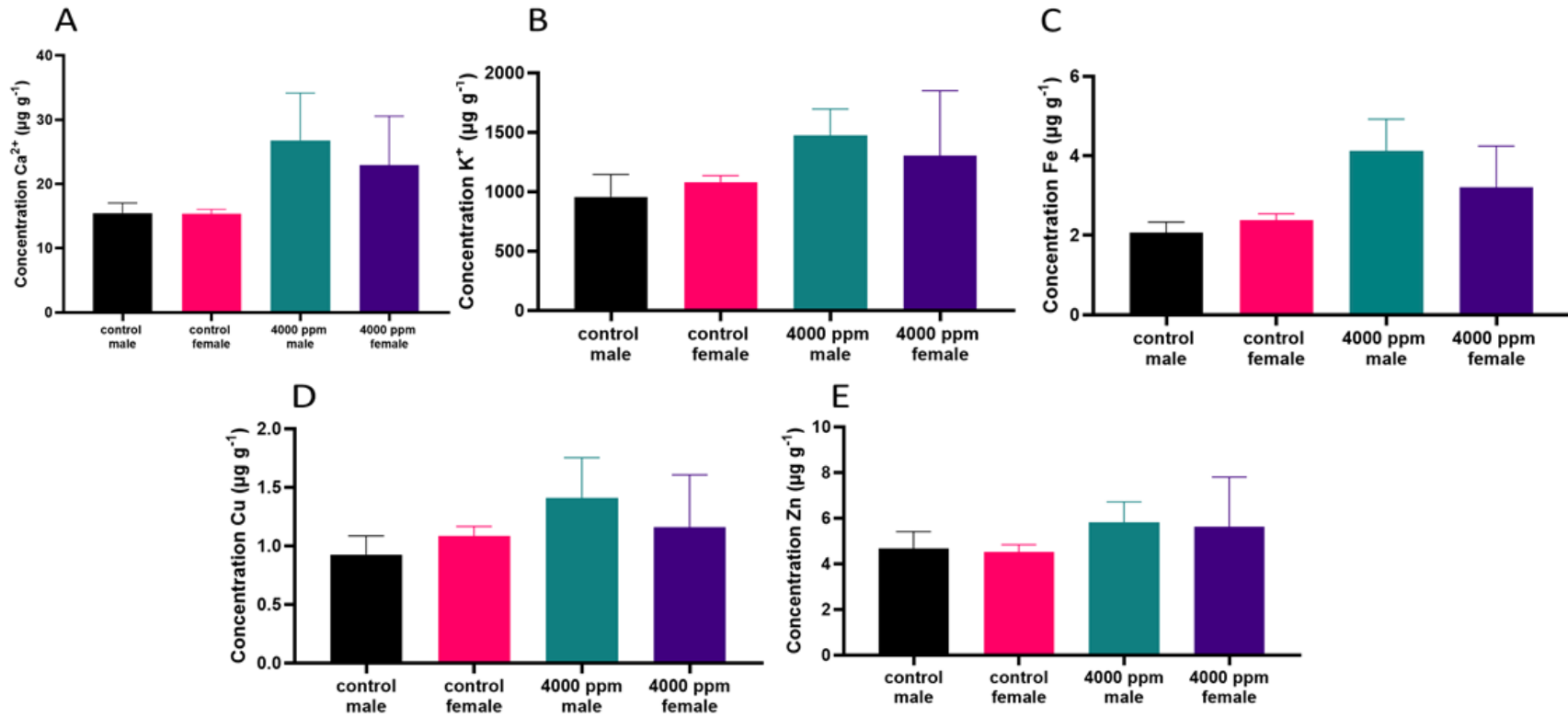


Figure 20. Comparisons of (A) calcium $p = 0.356$ (B) potassium $p = 0.694$ (C) iron $p = 0.187$ (D) copper $p = 0.386$ and (E) zinc $p = 0.859$ broken down by sex. No differences are significant.

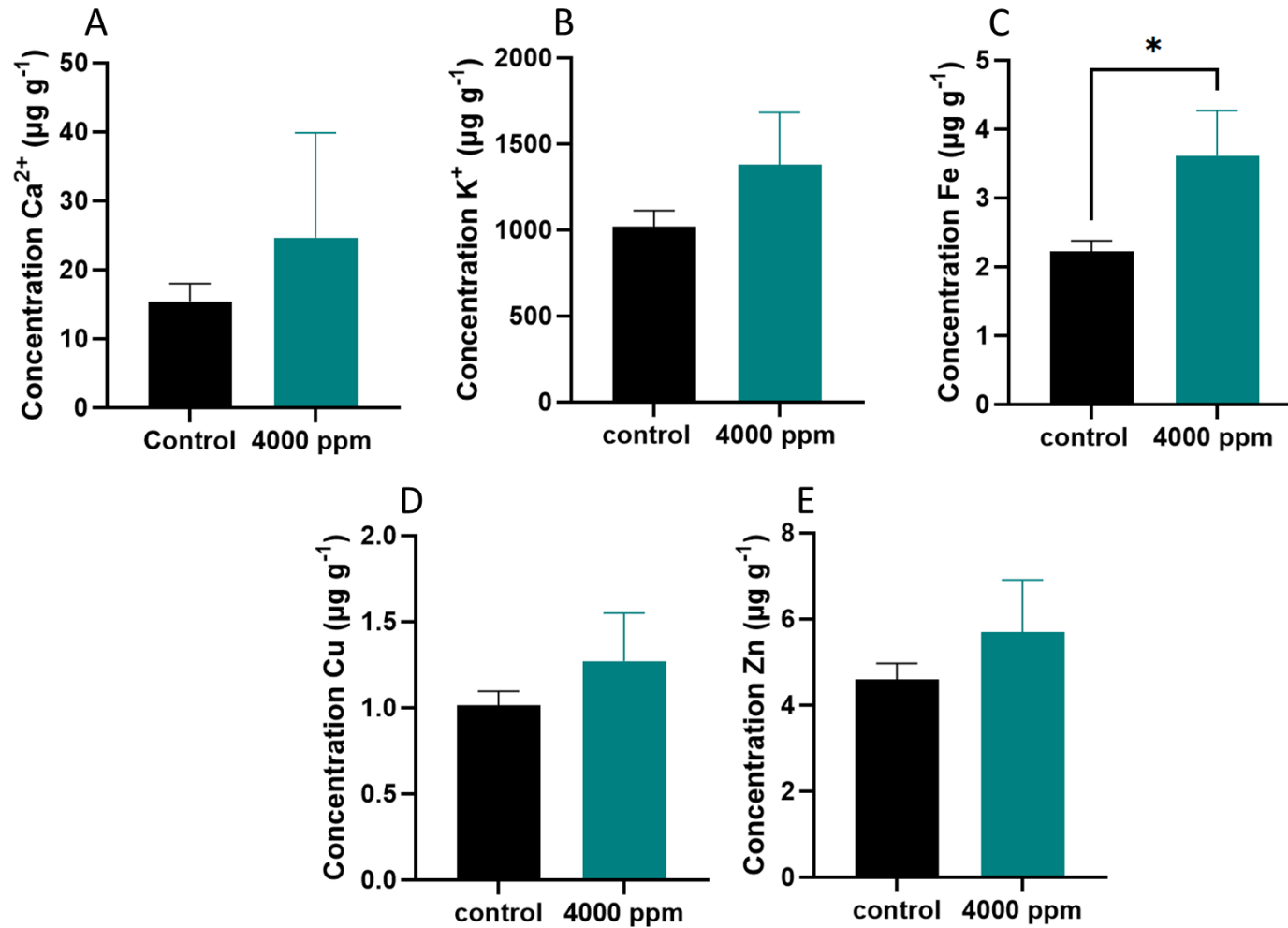


Figure 21. Concentration of (A) Calcium ($p=0.075$) (B) Potassium ($p=0.252$) (C) Iron $p=0.044$ (D) Copper ($p=0.386$), and (E) Zinc ($p=0.374$) from XRF analysis of nucleus accumbens biopsies. All comparisons were between 10 air control animals (5 males and 5 females except for copper where one male was removed by Q test) and 9 exposed animals (4 males and 5 females.)

CHAPTER 5

DISCUSSION

The present study endeavored to contribute understanding to possible compensatory mechanisms in the nucleus accumbens following chronic exposure to 2000 or 4000 ppm toluene. Previous studies have shown a decrease in evoked dopamine in the nucleus accumbens following 7 days of exposure, as well as suggesting that dopamine D3 receptor does not modulate the observed change (Apawu et al., 2020.) Here, the effect of chronic toluene exposure on dopamine release was verified, preliminary steps were taken to consider the possible involvement of Dopamine D2 receptors, and biometal analysis was used to infer possible mechanism.

5.1 Effect of Chronic Toluene Inhalation on Dopamine Release in the Nucleus Accumbens

This investigation confirmed the findings that chronic toluene exposure decreases dopamine release in the nucleus accumbens. When the data from males and females are considered separately, the control males released significantly more dopamine on average (344.8 nM) than the control females (76.53 nM), toluene-exposed males (42.80 nM) or the toluene-exposed females (41.60 nM). Previous studies have only examined male subjects and reported a reduction in evoked dopamine by approximately 40% (Apawu et al., 2020). The reduction seen here is 78-88%. While these data support previous findings that an overall decrease in evoked dopamine is observed, the difference in magnitude is notable. The difference between evoked dopamine release in control males and control females was not expected. Nevertheless, previous studies have established sex differences in dopaminergic neurons, such as neuroprotective factors of 17 β -estradiol and progesterone in the nigrostriatal pathway (Bourque et al., 2011), and

VMAT2 uptake rates (Dluzen et al., 2008). Furthermore, slice FSCV in the caudate nucleus of rats has shown greater dopamine release in females than males, even when accounting for estrous cycle (Walker et al., 1999). More recently chronoamperometry in the dorsal striatum of C57/BI6J (most common model in clinical research) mice also showed a larger dopamine release in females than males (Arvidsson et al., 2014). Thus, the observed difference in the dopamine release in the present work is not consistent with existing literature. Since it is possible that small adjustments to the software used for analysis can produce wide variance in results, the data analysis parameters were strictly chosen, and outlier data were not used. Furthermore, because electrodes may also introduce variability, calibration factors were determined after each experiment and used in analysis to eliminate variability between electrodes. Future work should explore the molecular basis underlying the difference in dopamine release between sexes.

5.2 The Possible Role of D2 Receptors in Toluene-Induced Changes in the Nucleus Accumbens

To investigate adaptation to chronic exposure and explore the role of D2 in possible compensation, the density of D2 receptors in the nucleus accumbens core and shell was mapped with immunocytochemistry and confocal microscopy. See appendix A for representative images. The results indicated there was no significant difference in D2 density between sexes or treatment conditions. A greater density of D2 receptors was observed in the nucleus accumbens core than the shell, which is consistent with literature (Bardo & Hammer, 1991). While specific functions governed by the core and shell are still being studied, the evidence from this study is consistent with differing functions between the two regions. Dopamine receptors in the nucleus accumbens core respond to constant baseline stimulation from the ventral tegmental area, whereas dopamine receptors in the shell respond to dynamic bursts and pauses in ventral tegmental area stimulation (Dreyer et al., 2016). Activation of D2 receptors only inhibit the

firing of certain dopaminergic projections from the ventral tegmental area (Roepers, 2013), while toluene is believed to increase the firing rate by acting on the intrinsic mechanisms that regulate firing, such as potassium ion channels (Woodward & Beckley, 2014).

There was no significant difference between the average density of D2 receptors in control and 4000 ppm toluene exposed mice. However, radiological evidence suggests that there are fewer available binding sites to D2 receptors after prolonged exposure to addictive stimuli and to compensate for this effect, more D2 proteins are expressed. In humans, significant differences in D2 receptors are seen in type I (late-life onset after prolonged, heavy drinking) but not type II (patrilateral adolescent onset) alcoholics (Tupala et al., 2003). If these differences accumulate over a lifespan, a seven-day exposure paradigm may not be sufficient to observe differences.

To further analyze if the same number of D2 receptors are present, but have undergone a change, for instance if there are different proportions of short and long splice variants, D2S and D2L, (Wang et al., 2000), techniques such as western blot or flow cytometry can be used. Preliminary investigation has shown complications with these techniques. Flow cytometry on neurons is not optimal, as the digestion process breaks off the long dendrites and axons from the cell body. The result is closer to analyzing cell lysate, not whole cells. Western blot lyses cells so their delicate nature is not an issue. However, biopsies of the nucleus accumbens are 1 milligram on average, and tissue preparation on a small-scale lead to ambiguous or negative results when staining. The literature documents methods to explore, such as using fixatives prior to flow cytometry (Martin et al., 2017) or investigating different antibodies to use for labeling.

5.3 The Role of Biometal Ion Cofactors in Toluene's Action on the Dopamine System

Cell signaling and response pathways are complex and frequently rely on ion secondary messengers. To further illuminate processes which may be affected by chronic toluene exposure, elemental analysis of cell lysates from nucleus accumbens biopsies was conducted by X-ray fluoresce.

Results showed greater concentration, as well as greater variability in concentration, of elements of interest in 4000 ppm toluene-exposed biopsies than in air control. This difference was only significant for iron where exposed concentrations averaged $3.613 \mu\text{g g}^{-1}$ and control averaged $2.218 \mu\text{g g}^{-1}$ ($t(17)= 2.171$ $p=0.044$). While Fe^{2+} is necessary for catalytic activity of tyrosine hydroxylase, literature suggests that phosphorylation to achieve the appropriate oxidation state of iron is the most prevalent mediator of tyrosine hydroxylase activity, not access to an iron ion itself (Frantom et al., 2006).

The observed increase in iron following exposure to drugs of abuse is consistent with literature. Exposure of macrophages to increased dopamine has been shown to increase the uptake of non-transferrin bound iron (Dichtl et al., 2018), which is thought to contribute the generation of reactive oxygen species and oxidative stress (Deavall et al., 2012). A study by Verma et al. (2017) of teenagers in Northern India who voluntarily inhaled toluene showed significantly elevated levels of superoxide dismutase in their urine samples, which is interpreted as evidence that their bodies were trying to maintain homeostasis against an increase in reactive oxygen species (ROS). The link between excessive production of ROS and drug addiction is widely known. In 2017 Jang et al. showed injections of ROS scavengers in rats mediated the effect of methamphetamine on excessive locomotion and several potential addiction therapies utilize antioxidants (Iida et al., 2017). Furthermore, ROS like hydrogen peroxide is known to

modulate synaptic dopamine neurotransmission by acting on ATP-sensitive K^+ channels (Avshalumov et al., 2005). Further investigation of oxidative stress may prove illuminating.

While there was no significant difference in potassium or calcium between treatment and control, this was a global analysis. Extracellular vs intracellular techniques would be necessary to answer if there was a specific effect on ion transport or binding of D2 $G_{\beta\gamma}$ to voltage gated Ca^{2+} channels.

This investigation analyzed the supernatant from cell lysates, but not the pellet. A common preparation technique in literature is to freeze dry tissue, dissolve the resulting particulates in acid, and then analyze the whole tissue sample by XRF or Proton Induced X-ray Emission (PIXE). Duflou et al., (1989) using the aforementioned preparation and PIXE report μg of element per g of wet tissue concentrations for potassium and calcium in gray and mixed matter samples of whole tissue human brain samples that are 2.31x and 2.70x greater respectively than what is reported here. Both Duflou et al. and Zheng et al. (2012), the latter using XRF, reported values of iron in the 35-45 $\mu\text{g g}^{-1}$ range, which is 13.6 times greater than what was observed in this investigation data. The value reported by Duflou et al. for copper was 7.1x greater than what was found in the present analysis. The literature value for zinc is 23 $\mu\text{g g}^{-1}$ in white matter generally, as reported by (Zheng et al., 2012.) This investigation reported an average of 5.12 $\mu\text{g g}^{-1}$. Considering the present investigation only analyzed the supernatant, future steps could include resuspending the pellet, or creating a homogenized lysate for direct comparison.

Copper is highly localized to the substantia nigra and a necessary enzymatic cofactor in the synthesis of norepinephrine from dopamine (Davies et al., 2013). Additionally, copper or zinc $2+$ cations are required cofactors for superoxide dismutase. An excess of copper has been associated with neurodegenerative disorders such as Parkinson's and Huntington's, but the

mechanism is still not well understood (Loeffler et al., 1996). Zinc is widely distributed in the brain and even mild deficiency impairs brain function (Doboszewska et al., 2017). Zinc can act in many neurological capacities. Zinc is a cofactor to enzymes, such as activating certain G coupled Protein Receptors, inhibiting the dopamine transporter (DAT), and capable of modulating antagonistic binding of all D2 like receptors (Schetz et al., 1999.) Additionally, zinc can act as a neurotransmitter itself, undergoing vesicle packaging and deployment (Doboszewska et al., 2017).

Overall, the difference in iron content is intriguing, but to make meaningful conclusions from the other elements analyzed would require knowing other details, such as their location inside or outside of the neuron. Different preparation may yield results more consistent with literature or produce more significant trends.

5.4 Conclusion

This investigation confirmed previous reports of diminished dopamine release following chronic exposure to 4000 ppm toluene. The sex differences in dopamine release observed in this research may indicate that neuroprotective factors like 17β -estradiol and progesterone, or sex-based differences like VMAT2 uptake rates, interact with toluene directly.

The density of D2 receptors was not significantly different after chronic exposure to 2000 or 4000 ppm toluene. Transcription factors are affected by exposure to salient stimuli and future investigations may explore longer exposure paradigms to look for a more subtle effect of continued exposure. In addition, future work may utilize different approaches, such as flow cytometry or western blot, to gain additional information regarding dopamine receptor 2 levels.

XRF data showed significantly more iron in the nucleus accumbens of mice chronically exposed to 4000 ppm toluene. In addition, analysis of whole tissue can be used to support findings of lysate analysis. While an increase in iron itself may not directly impact dopamine

synthesis, the oxidation state of the iron can deplete catalytic function. Tetrahydrobiopterin and phosphokinases activate tyrosine hydroxylase and ensure it is redox active. If extraneous iron atoms are competitively inhibiting the ability of tetrahydrobiopterin and phosphokinases to activate tyrosine hydroxylase, then dopamine synthesis could be decreased. Analysis of the oxidation state of iron is a possible avenue for future analysis. Combined with clinical evidence of oxidative stress following exposure to toluene, further investigation of reactive oxygen species' interaction with dopamine receptors may prove illuminating.

REFERENCES

- Adinoff, B. (2004). Neurobiologic Processes in Drug Reward and Addiction. *Harvard Review of Psychiatry*, 12(6), 305–320. <https://doi.org/10.1080/10673220490910844>
- Apawu, A. K., Callan, S. P., Matthews, T. A., & Bowen, S. E. (2020). Repeated Toluene Exposure Leads to Neuroadaptation in Dopamine Release Mechanisms within the Nucleus Accumbens Core. *Toxicology and Applied Pharmacology* 408: 115260. <https://doi.org/10.1016/j.taap.2020.115260>.
- Apawu, A. K., Mathews, T. A., & Bowen, S. E. (2015). Striatal dopamine dynamics in mice following acute and repeated toluene exposure. *Psychopharmacology*, 232(1), 173–184. <https://doi.org/10.1007/s00213-014-3651-x>
- Arvidsson, E., Viereckel, T., Mikulovic, S., & Wallén-Mackenzie, Å. (2014). Age- and Sex-Dependence of Dopamine Release and Capacity for Recovery Identified in the Dorsal Striatum of C57/Bl6J Mice.” *PLOS ONE* 9, no. 6 e99592. <https://doi.org/10.1371/journal.pone.0099592>.
- Avshalumov, M. V., Chen, B. T., Koós, T., Tepper, J. M., & Rice, M. E. (2005). Endogenous Hydrogen Peroxide Regulates the Excitability of Midbrain Dopamine Neurons via ATP-Sensitive Potassium Channels. *Journal of Neuroscience*, 25(17), 4222–4231. <https://doi.org/10.1523/JNEUROSCI.4701-04.2005>
- Bardo, M. T., & Hammer, R. P. (1991). Autoradiographic localization of dopamine D1 and D2 receptors in rat nucleus accumbens: Resistance to differential rearing conditions. *Neuroscience*, 45(2), 281–290. [https://doi.org/10.1016/0306-4522\(91\)90226-E](https://doi.org/10.1016/0306-4522(91)90226-E)

- Barron, A. B., Søvik, E., & Cornish, J. L. (2010). The Roles of Dopamine and Related Compounds in Reward-Seeking Behavior Across Animal Phyla. *Frontiers in Behavioral Neuroscience*, 4. <https://doi.org/10.3389/fnbeh.2010.00163>
- Beaulieu, J.-M., & Gainetdinov, R. R. (2011). The Physiology, Signaling, and Pharmacology of Dopamine Receptors. *Pharmacological Reviews*, 63(1), 182–217. <https://doi.org/10.1124/pr.110.002642>
- Biga, L. M., Dawson, S., Harwell, A., Hopkins, R., Kaufmann, J., LeMaster, M., Matern, P., Morrison-Graham, K., Quick, D., & Runyeon, J. (2019). 12.5 The Action Potential. In *Anatomy & Physiology*. OpenStax/Oregon State University. <https://open.oregonstate.edu/aandp/chapter/12-5-the-action-potential/>
- Bourque, M., Dluzen, D. E., & Di Paolo, T. (2011). Male/Female Differences in Neuroprotection and Neuromodulation of Brain Dopamine. *Frontiers in Endocrinology*, 2. <https://doi.org/10.3389/fendo.2011.00035>
- Bowen, S. E., Batis, J. C., Paez-Martinez, N., & Cruz, S. L. (2006). The last decade of solvent research in animal models of abuse: Mechanistic and behavioral studies. *Neurotoxicology and Teratology*, 28(6), 636–647. <https://doi.org/10.1016/j.ntt.2006.09.005>
- Brini, M., Calì, T., Ottolini, D., & Carafoli, E. (2014). Neuronal calcium signaling: Function and dysfunction. *Cellular and Molecular Life Sciences: CMLS*, 71(15), 2787–2814. <https://doi.org/10.1007/s00018-013-1550-7>
- Camara-Lemarroy, C. R., Rodríguez-Gutiérrez, R., Monreal-Robles, R., & González-González, J. G. (2015). Acute toluene intoxication—clinical presentation, management and prognosis: a prospective observational study. *BMC Emergency Medicine*, 15. <https://doi.org/10.1186/s12873-015-0039-0>

- Cruz, S. L., Rivera-García, M. T., & Woodward, J. J. (2014). Review of toluene action: clinical evidence, animal studies and molecular targets. *Journal of Drug and Alcohol Research*, 3. <https://doi.org/10.4303/jdar/235840>
- Davies, K. M., Hare, D. J., Cottam, V., Chen, N., Hilgers, L., Halliday, G., Mercer, J. F. B., & Double, K. L. (2013). Localization of copper and copper transporters in the human brain. *Metallomics: Integrated Biometal Science*, 5(1), 43–51. <https://doi.org/10.1039/c2mt20151h>
- Deavall, D. G., Martin, E. A., Horner, J. M., & Roberts, R. (2012). Drug-Induced Oxidative Stress and Toxicity. *Journal of Toxicology*, 2012, e645460. <https://doi.org/10.1155/2012/645460>
- Denker, A., & Rizzoli, S. O. (2010). Synaptic Vesicle Pools: An Update. *Frontiers in Synaptic Neuroscience*, 2. <https://doi.org/10.3389/fnsyn.2010.00135>
- Dichtl, S., Haschka, D., Nairz, M., Seifert, M., Volani, C., Lutz, O., & Weiss, G. (2018). Dopamine promotes cellular iron accumulation and oxidative stress responses in macrophages. *Biochemical Pharmacology*, 148, 193–201. <https://doi.org/10.1016/j.bcp.2017.12.001>
- Dluzen, D. E., Bhatt, S., & McDermott, J. L. (2008). Differences in reserpine-induced striatal dopamine output and content between female and male mice: Implications for sex differences in vesicular monoamine transporter 2 function. *Neuroscience*, 154(4), 1488–1496. <https://doi.org/10.1016/j.neuroscience.2008.04.051>
- Doboszewska, U., Wlaź, P., Nowak, G., Radziwoń-Zaleska, M., Cui, R., & Młyniec, K. (2017). Zinc in the Monoaminergic Theory of Depression: Its Relationship to Neural Plasticity. *Neural Plasticity*, 2017. <https://doi.org/10.1155/2017/3682752>

- Dong, N., Lee, D. W. K., Sun, H.-S., & Feng, Z.-P. (2018). Dopamine-mediated calcium channel regulation in synaptic suppression in *L. stagnalis* interneurons. *Channels*, *12*(1), 153–173. <https://doi.org/10.1080/19336950.2018.1457897>
- Dreyer, J. K., Vander Weele, C. M., Lovic, V., & Aragona, B. J. (2016). Functionally Distinct Dopamine Signals in Nucleus Accumbens Core and Shell in the Freely Moving Rat. *The Journal of Neuroscience*, *36*(1), 98–112. <https://doi.org/10.1523/JNEUROSCI.2326-15.2016>
- Duflou, H., Maenhaut, W., & De Reuck, J. (1989). Regional distribution of potassium, calcium, and six trace elements in normal human brain. *Neurochemical Research*, *14*(11), 1099–1112. <https://doi.org/10.1007/BF00965616>
- Filley, C. M., Halliday, W., & Kleinschmidt-DeMasters, B. K. (2004). The Effects of Toluene on the Central Nervous System. *Journal of Neuropathology and Experimental Neurology; Cary*, *63*(1), 1–12.
- Frantom, P. A., Seravalli, J., Ragsdale, S. W., & Fitzpatrick, P. F. (2006). Reduction and Oxidation of the Active Site Iron in Tyrosine Hydroxylase: Kinetics and Specificity. *Biochemistry*, *45*(7), 2372–2379. <https://doi.org/10.1021/bi052283j>
- Fujisawa, H., & Okuno, S. (2005). Regulatory mechanism of tyrosine hydroxylase activity. *Biochemical and Biophysical Research Communications*, *338*(1), 271–276. <https://doi.org/10.1016/j.bbrc.2005.07.183>
- Goodwin, J. S., Larson, G. A., Swant, J., Sen, N., Javitch, J. A., Zahniser, N. R., De Felice, L. J., Khoshbouei, H. (2009). Amphetamine and Methamphetamine Differentially Affect Dopamine Transporters in Vitro and in Vivo. *The Journal of Biological Chemistry*, *284*(5), 2978–2989. <https://doi.org/10.1074/jbc.M805298200>

- Grochowski, C., Blicharska, E., Krukow, P., Jonak, K., Maciejewski, M., Szczepanek, D., Jonak, K., Flieger, J., & Maciejewski, R. (2019). Analysis of Trace Elements in Human Brain: Its Aim, Methods, and Concentration Levels. *Frontiers in Chemistry*, 7. <https://doi.org/10.3389/fchem.2019.00115>
- Hillas, P. J., & Fitzpatrick, P. F. (1996). A mechanism for hydroxylation by tyrosine hydroxylase based on partitioning of substituted phenylalanines. *Biochemistry*, 35(22), 6969–6975. <https://doi.org/10.1021/bi9606861>
- Iida, T., Yi, H., Liu, S., Ikegami, D., Zheng, W., Liu, Q., Takahashi, K., Kashiwagi, Y., Goins, W. F., Glorioso, J. C., & Hao, S. (2017). MnSOD mediated by HSV vectors in the periaqueductal gray suppresses morphine withdrawal in rats. *Gene Therapy*, 24(5), 314–324. <https://doi.org/10.1038/gt.2017.22>
- Jang, E. Y., Yang, C. H., Hedges, D. M., Kim, S. P., Lee, J. Y., Ekins, T. G., Garcia, B. T., Kim, H. Y., Nelson, A. C., Kim, N. J., & Steffensen, S. C. (2017). The role of reactive oxygen species in methamphetamine self-administration and dopamine release in the nucleus accumbens. *Addiction Biology*, 22(5), 1304–1315. <https://doi.org/10.1111/adb.12419>
- Le Foll, B., Goldberg, S. R., & Sokoloff, P. (2005). The dopamine D3 receptor and drug dependence: Effects on reward or beyond? *Neuropharmacology*, 49(4), 525–541. <https://doi.org/10.1016/j.neuropharm.2005.04.022>
- Lim, D. H., LeDue, J., Mohajerani, M. H., Vanni, M. P., & Murphy, T. H. (2013). Optogenetic approaches for functional mouse brain mapping. *Frontiers in Neuroscience*, 7. <https://doi.org/10.3389/fnins.2013.00054>
- Loeffler, D. A., LeWitt, P. A., Juneau, P. L., Sima, A. A., Nguyen, H. U., DeMaggio, A. J., Brickman, C. M., Brewer, G. J., Dick, R. D., Troyer, M. D., & Kanaley, L. (1996).

- Increased regional brain concentrations of ceruloplasmin in neurodegenerative disorders. *Brain Research*, 738(2), 265–274. [https://doi.org/10.1016/s0006-8993\(96\)00782-2](https://doi.org/10.1016/s0006-8993(96)00782-2)
- Madras, B., & Kuhar, M. (2014). *The Effects of Drug Abuse on the Human Nervous System*. <https://doi.org/10.1016/C2013-0-09757-5>
- Martin, D., Xu, J., Porretta, C., & Nichols, C. D. (2017). Neurocytometry: Flow cytometric sorting of specific neuronal populations from human and rodent brain. *ACS Chemical Neuroscience*, 8(2), 356–367. <https://doi.org/10.1021/acschemneuro.6b00374>
- Mishra, A., Singh, S., & Shukla, S. (2018). Physiological and Functional Basis of Dopamine Receptors and Their Role in Neurogenesis: Possible Implication for Parkinson's disease. *Journal of Experimental Neuroscience*, 12. <https://doi.org/10.1177/1179069518779829>
- Morgan, D., Grant, K. A., Gage, H. D., Mach, R. H., Kaplan, J. R., Prioleau, O., Nader S. H., Bruchheimer, N., Ehrenkauf, R. L., & Nader, M. A. (2002). Social dominance in monkeys: dopamine D2 receptors and cocaine self-administration. *Nature Neuroscience*, 5(2), 169. <https://doi.org/10.1038/nn798>
- Nagel, G., Brauner, M., Liewald, J. F., Adeishvili, N., Bamberg, E., & Gottschalk, A. (2005). Light activation of channelrhodopsin-2 in excitable cells of *Caenorhabditis elegans* triggers rapid behavioral responses. *Current Biology: CB*, 15(24), 2279–2284. <https://doi.org/10.1016/j.cub.2005.11.032>
- National Institute on Drug Abuse. (2011). *What are inhalants?* <https://www.drugabuse.gov/publications/research-reports/inhalants/what-are-inhalants>
- National Institute on Drug Abuse. (2016). *How does cocaine produce its effects?* <https://www.drugabuse.gov/publications/research-reports/cocaine/how-does-cocaine-produce-its-effects>

- Ortiz, A. N., Kurth, B. J., Osterhaus, G. L., & Johnson, M. A. (2010). Dysregulation of intracellular dopamine stores revealed in the R6/2 mouse striatum. *Journal of Neurochemistry*, *112*(3), 755–761. <https://doi.org/10.1111/j.1471-4159.2009.06501.x>
- Paxinos, G., & Franklin, K. B. J. (2001). *The mouse brain in stereotaxic coordinates* (2nd ed). Academic.
- Pierce, R. C., & Kumaresan, V. (2006). The mesolimbic dopamine system: The final common pathway for the reinforcing effect of drugs of abuse? *Neuroscience & Biobehavioral Reviews*, *30*(2), 215–238. <https://doi.org/10.1016/j.neubiorev.2005.04.016>
- Puig, M. V., Rose, J., Schmidt, R., & Freund, N. (2014). Dopamine modulation of learning and memory in the prefrontal cortex: insights from studies in primates, rodents, and birds. *Frontiers in Neural Circuits*, *8*. <https://doi.org/10.3389/fncir.2014.00093>
- Ramakrishnan, N. A., Drescher, M. J., & Drescher, D. G. (2012). The SNARE complex in neuronal and sensory cells. *Molecular and Cellular Neurosciences*, *50*(1), 58–69. <https://doi.org/10.1016/j.mcn.2012.03.009>
- Ramsey, A. J., Hillas, P. J., & Fitzpatrick, P. F. (1996). Characterization of the Active Site Iron in Tyrosine Hydroxylase: REDOX STATES OF THE IRON *. *Journal of Biological Chemistry*, *271*(40), 24395–24400. <https://doi.org/10.1074/jbc.271.40.24395>
- Riegel, A. C., & French, E. D. (1999). An electrophysiological analysis of rat ventral tegmental dopamine neuronal activity during acute toluene exposure. *Pharmacology & Toxicology*, *85*(1), 37–43.
- Riegel, A. C., Zapata, A., Shippenberg, T. S., & French, E. D. (2007). The Abused Inhalant Toluene Increases Dopamine Release in the Nucleus Accumbens by Directly Stimulating

Ventral Tegmental Area Neurons. *Neuropsychopharmacology*, 32(7), 1558–1569.

<https://doi.org/10.1038/sj.npp.1301273>

Roberts, J. G., & Sombers, L. A. (2018). Fast-Scan Cyclic Voltammetry: Chemical Sensing in the Brain and Beyond. *Analytical Chemistry*, 90(1), 490–504.

<https://doi.org/10.1021/acs.analchem.7b04732>

Robison, A. J., & Nestler, E. J. (2011). Transcriptional and epigenetic mechanisms of addiction.

Nature Reviews Neuroscience, 12(11), 623–637. <https://doi.org/10.1038/nrn3111>

Roeper, J. (2013). Dissecting the diversity of midbrain dopamine neurons. *Trends in*

Neurosciences, 36(6), 336–342. <https://doi.org/10.1016/j.tins.2013.03.003>

Schetz, J. A., Chu, A., & Sibley, D. R. (1999). Zinc Modulates Antagonist Interactions with D2-

Like Dopamine Receptors through Distinct Molecular Mechanisms. *Journal of*

Pharmacology and Experimental Therapeutics, 289(2), 956–964.

Scimemi, A., & Beato, M. (2009). Determining the Neurotransmitter Concentration Profile at

Active Synapses. *Molecular Neurobiology*, 40(3), 289–306.

<https://doi.org/10.1007/s12035-009-8087-7>

Substance Abuse and Mental Health Services Administration. (2018). *Key substance use and mental health indicators in the United States: Results from the 2017 National Survey on*

Drug Use and Health (HHS Publication No. SMA 18-5068, NSDUH Series H-53).

Rockville, MD: Center for Behavioral Health Statistics and Quality, Substance Abuse

and Mental Health Services Administration. Retrieved

from <https://www.samhsa.gov/data/>

- Substance Abuse and Mental Health Services Administration, Center for Behavioral Health Statistics and Quality. (July 17, 2014). The TEDS Report: Age of Substance Use Initiation among Treatment Admissions Aged 18 to 30. Rockville, MD.
- Südhof, T. C. (2012). Calcium Control of Neurotransmitter Release. *Cold Spring Harbor Perspectives in Biology*, 4(1). <https://doi.org/10.1101/cshperspect.a011353>
- Tang, J., Maximov, A., Shin, O.-H., Dai, H., Rizo, J., & Südhof, T. C. (2006). A Complexin/Synaptotagmin 1 Switch Controls Fast Synaptic Vesicle Exocytosis. *Cell*, 126(6), 1175–1187. <https://doi.org/10.1016/j.cell.2006.08.030>
- Thanos, P. K., Volkow, N. D., Freimuth, P., Umegaki, H., Ikari, H., Roth, G., ... Hitzemann, R. (2001). Overexpression of dopamine D2 receptors reduces alcohol self-administration. *Journal of Neurochemistry*, 78(5), 1094–1103. <https://doi.org/10.1046/j.1471-4159.2001.00492.x>
- Tupala, E., Hall, H., Mantere, T., Räsänen, P., Särkioja, T., & Tiihonen, J. (2003). Dopamine receptors and transporters in the brain reward circuits of type 1 and 2 alcoholics measured with human whole hemisphere autoradiography☆. *NeuroImage*, 19(1), 145–155. [https://doi.org/10.1016/S1053-8119\(03\)00060-0](https://doi.org/10.1016/S1053-8119(03)00060-0)
- Venton, B. J., Seipel, A. T., Phillips, P. E. M., Wetsel, W. C., Gitler, D., Greengard, P., Augustine, G. J., & Wightman, R. M. (2006). Cocaine Increases Dopamine Release by Mobilization of a Synapsin-Dependent Reserve Pool. *The Journal of Neuroscience*, 26(12), 3206. <https://doi.org/10.1523/JNEUROSCI.4901-04.2006>
- Verma, A., Jain, R., Dhawan, A., & Lakshmy, R. (2017). 34—Evaluation of oxidative stress and toluene exposure among adolescent inhalant users at a tertiary care centre of North India.

Free Radical Biology and Medicine, 112, 37.

<https://doi.org/10.1016/j.freeradbiomed.2017.10.047>

Villano, J. (2013, October 28). Inhalant Abuse | California Poison Control System | UCSF.

Retrieved May 13, 2019, from <https://calpoison.org/news/inhalant-abuse>

Volkow, N. D., Fowler, J. S., Wang, G. J., Baler, R., & Telang, F. (2009). Imaging dopamine's role in drug abuse and addiction. *Neuropharmacology*, 56 Suppl 1, 3–8.

<https://doi.org/10.1016/j.neuropharm.2008.05.022>

Volkow, N. D., Wang, G.-J., Begleiter, H., Porjesz, B., Fowler, J. S., Telang, F., Wong, C., Ma, Y., Logan, J., Goldstein, R., Alexoff, D., & Thanos, P. K. (2006). High levels of dopamine D2 receptors in unaffected members of alcoholic families: Possible protective factors. *Archives of General Psychiatry*, 63(9), 999–1008.

<https://doi.org/10.1001/archpsyc.63.9.999>

Volkow, N. D., Wang, G.-J., Fowler, J. S., Logan, J., Gatley, S. J., Gifford, A., Hitzemann, R., Ding, Y. S., & Pappas, N. (1999). Prediction of Reinforcing Responses to Psychostimulants in Humans by Brain Dopamine D2 Receptor Levels. *American Journal of Psychiatry*, 156(9), 1440–1443. <https://doi.org/10.1176/ajp.156.9.1440>

Walker, Q. D., Rooney, M. B., Wightman, R. M., & Kuhn, C. M. (1999). Dopamine release and uptake are greater in female than male rat striatum as measured by fast cyclic voltammetry. *Neuroscience*, 95(4), 1061–1070. [https://doi.org/10.1016/S0306-4522\(99\)00500-X](https://doi.org/10.1016/S0306-4522(99)00500-X)

Wang, Y., Xu, R., Sasaoka, T., Tonegawa, S., Kung, M. P., & Sankoorikal, E. B. (2000).

Dopamine D2 long receptor-deficient mice display alterations in striatum-dependent

functions. *The Journal of Neuroscience: The Official Journal of the Society for Neuroscience*, 20(22), 8305–8314.

Wirth, K., & Barth, A. (2020). *X-Ray Fluorescence (XRF) Techniques*.

https://serc.carleton.edu/research_education/geochemsheets/techniques/XRF.html

Woodward, J. J., & Beckley, J. (2014). Effects of the abused inhalant toluene on the mesolimbic dopamine system. *Journal of Drug and Alcohol Research*, 3.

<https://doi.org/10.4303/jdar/235838>

Zheng, W., Haacke, E. M., Webb, S. M., & Nichol, H. (2012). Imaging of stroke: A comparison between X-ray fluorescence and magnetic resonance imaging methods. *Magnetic*

Resonance Imaging, 30(10), 1416–1423. <https://doi.org/10.1016/j.mri.2012.04.011>

APPENDIX A
IMMUNOCYTOCHEMISTRY IMAGES

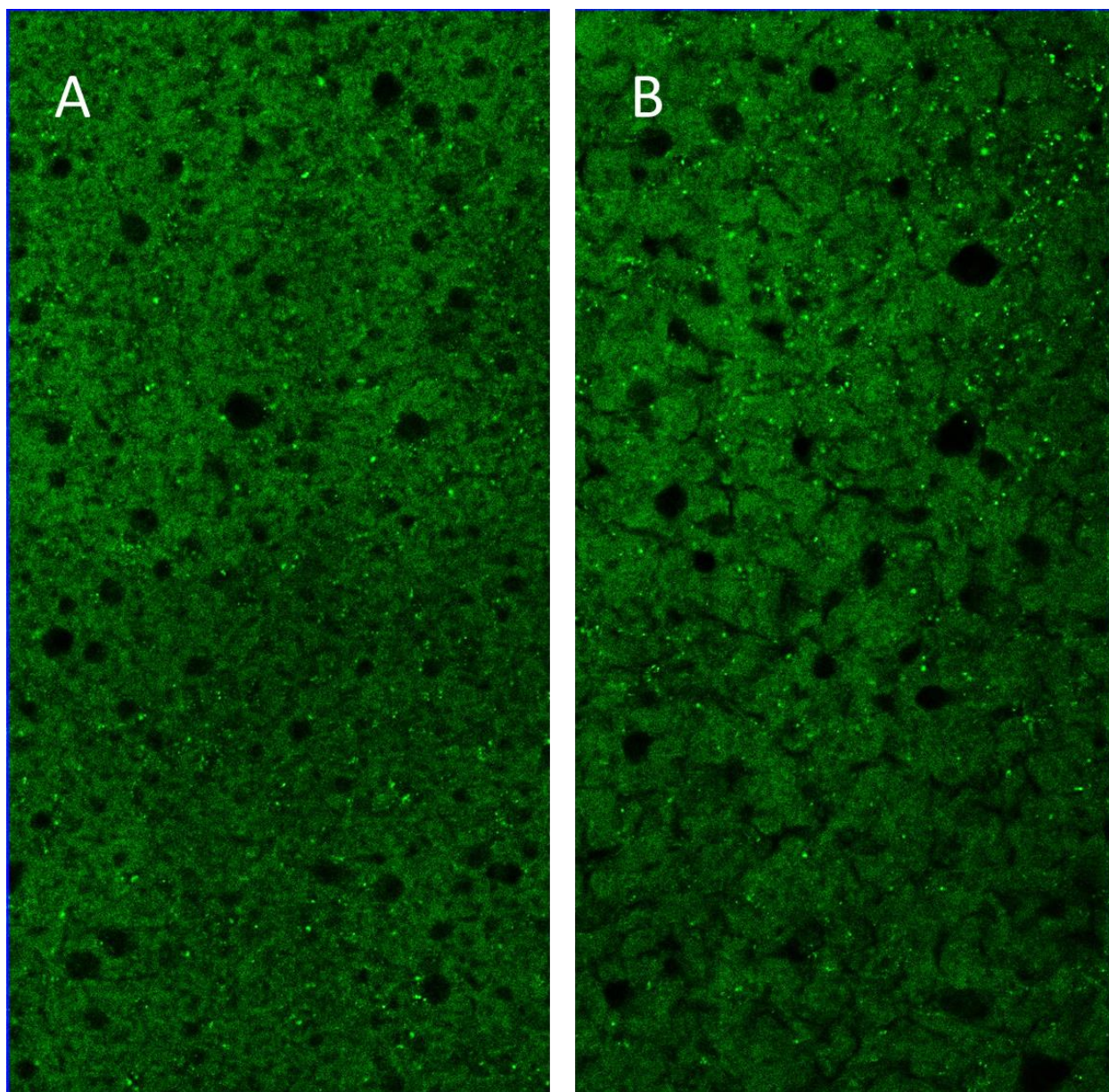


Figure 22: Representative ICC staining of (A) control male and (B) 4000 ppm exposed male nucleus accumbens core. Both images measure 300 μm wide by 600 μm tall.

APPENDIX B

INSTITUTIONAL ANIMAL CARE AND
USE COMMITTEE APPROVAL



IACUC Memorandum

To: Aaron Apawu

From: Laura Martin, Director of Compliance and Operations, ARF

CC: IACUC Files

Date: September 26, 2019

Re: IACUC Protocol 1908CD-AA-M-22 Approval

The UNC IACUC has completed a final review of your protocol “Elucidating the neurochemical basis underlying the effect of inhalants (toluene) on the mesolimbic dopamine systems”. The protocol review was based on the requirements of Government Principles for the Utilization and Care of Vertebrate Animals Used in Testing, Research, and Training; the Public Health Policy on Humane Care and Use of Laboratory Animals; and the USDA Animal Welfare Act and Regulations. Based on the review, the IACUC has determined that all review criteria have been adequately addressed. The PI/PD is approved to perform the experiments or procedures as described in the identified protocol as submitted to the Committee. This protocol has been assigned the following number 1908CD-AA-M-22.

The next annual review will be due before September 26, 2020.

Sincerely,

A handwritten signature in black ink, appearing to read "Laura Martin", is positioned above a solid horizontal line that spans the width of the signature.

Laura Martin, Director of Compliance and Operations